

AD-A125 024

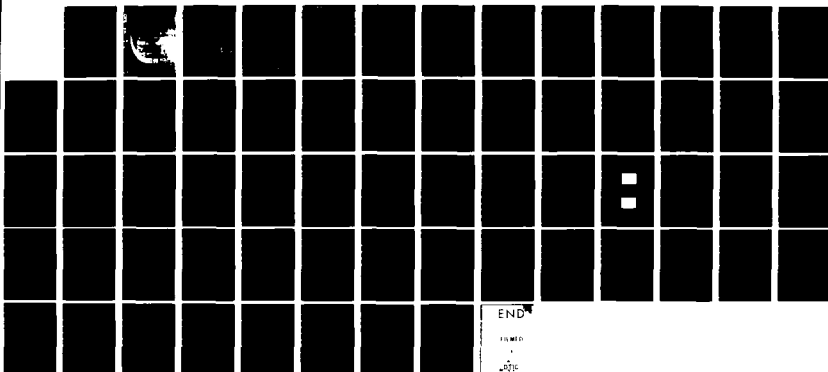
CURRENT INTERRUPTION AND PARTICLE BEAM GENERATION BY A
PLASMA FOCUS(U) ILLINOIS UNIV AT URBANA FUSION STUDIES
LAB G GERDIN ET AL. 30 NOV 82 FSL-102 AFOSR-TR-83-0037
AFOSR-79-0121

1/1

UNCLASSIFIED

F/G 20/7

NL

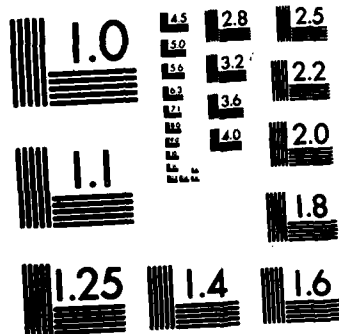


END

UNRECORDED

DATE

TIME



MICROCOPY RESOLUTION TEST CHART
NATIONAL BUREAU OF STANDARDS-1963-A

3

AD A125024

WIL FILE COPY



LABORATORY

Nuclear Engineering Program
University of Illinois
Urbana, Illinois 61801

Approved for public release
Distribution unlimited

83-02-028-031

Interim Annual Report FSL-102 ✓
30 Sept. 1981 - 30 Sept. 1982

Current Interruption and Particle Beam
Generation by a Plasma Focus

Glenn Gerdin and Francesco Venneri

Fusion Studies Laboratory
214 Nuclear Engineering Lab.
103 S. Goodwin
University of Illinois
Urbana, Illinois 61801

DTIC
ELECTE
S FEB 28 1983 D
B

AIR FORCE OFFICE OF SCIENTIFIC RESEARCH (AFSC)
NOTICE OF TRANSMITTAL TO DTIC
This technical report has been reviewed and is
approved for public release IAW AFR 190-12.
Distribution is unlimited.
MATTHEW J. KERPER
Chief, Technical Information Division

DISTRIBUTION STATEMENT A
Approved for public release;
Distribution Unlimited

TABLE OF CONTENTS

	<u>Page</u>
Title Page	i
Table of Contents.	ii
Report Documentation Page (DOD Form DD 1473)	iii
a) Abstract	1
b) Research Objectives 1981-82.	2
c) Status of Plasma Focus Opening Switch Research	2
1) Overview.	2
2) Soft X-ray Analysis of a Dense Plasma Focus	5
3) Theoretical and Computational Effort.	11
4) Summary of Particle Beam Scaling Measurements	13
5) References to main text	18
6) Figures for main text	21
7) Appendix A.	38
8) References for Appendix A	43
9) Figures for Appendix A.	44
10) Appendix B.	46
11) References for Appendix B	53
12) Table B1.	54
13) Figure B1	55
d) Cumulative Chronological List of Publications.	56
e) List of Personnel.	56
f) Interactions	57



Accession For	
NTIS GRA&I	<input checked="" type="checkbox"/>
DTIC TAB	<input type="checkbox"/>
Unannounced	<input type="checkbox"/>
Justification	
By _____	
Distribution/	
Availability Codes	
Dist	Avail and/or Special
A	

UNCLASSIFIED

111

SECURITY CLASSIFICATION OF THIS PAGE (When Data Entered)

REPORT DOCUMENTATION PAGE		READ INSTRUCTIONS BEFORE COMPLETING FORM
1. REPORT NUMBER AFOSR-TR- 83-0037	2. GOVT ACCESSION NO. AD-A125024	3. RECIPIENT'S CATALOG NUMBER
4. TITLE (and Subtitle) Current Interruption and Particle Beam Generation by a Plasma Focus		5. TYPE OF REPORT & PERIOD COVERED Interim Annual Report 30 Sept. 1981-30 Sept. 1982
		6. PERFORMING ORG. REPORT NUMBER
7. AUTHOR(s) Glenn Gerdin and Francesco Venneri		8. CONTRACT OR GRANT NUMBER(s) AFOSR-79-0121
9. PERFORMING ORGANIZATION NAME AND ADDRESS Fusion Studies Laboratory, Illinois University 214 Nuclear Engineering Lab 103 S. Goodwin, Urbana, IL 61801		10. PROGRAM ELEMENT, PROJECT, TASK AREA & WORK UNIT NUMBERS 61102F 2301/A7
11. CONTROLLING OFFICE NAME AND ADDRESS Air Force Office of Scientific Research /MP Bldg. 410, Bolling AFB, Washington, D.C. 20332		12. REPORT DATE Nov. 30, 1982
		13. NUMBER OF PAGES 61
14. MONITORING AGENCY NAME & ADDRESS (if different from Controlling Office)		15. SECURITY CLASS. (of this report) Unclassified
		15a. DECLASSIFICATION/DOWNGRADING SCHEDULE
16. DISTRIBUTION STATEMENT (of this Report) Approved for public release, distribution unlimited		
17. DISTRIBUTION STATEMENT (of the abstract entered in Block 20, if different from Report)		
18. SUPPLEMENTARY NOTES		
19. KEY WORDS (Continue on reverse side if necessary and identify by block number) Dense Plasma Focus Repetitive Opening Switch Soft X-ray Diagnostics Particle Beam Generation		
20. ABSTRACT (Continue on reverse side if necessary and identify by block number) Through collaboration with Dr. K. H. Schoenbach of Texas Tech University the plasma focus opening switch (PFOS) was revised to answer basic questions as to the utility of the concept. To estimate the plasma temperature and classical resistivity a soft X-ray spectrometer and X-ray pinhole camera were developed. The temperature was estimated from a coronal model to range between 0.4 to 0.5 keV for either a nitrogen or neon impurity (1 to 2%) in deuterium at 3 torr. Strong pinches were observed in pure (Please see other side of page)		

DD FORM 1473
1 JAN 73EDITION OF 1 NOV 68 IS OBSOLETE
S/N 0102-014-6601

UNCLASSIFIED

SECURITY CLASSIFICATION OF THIS PAGE (When Data Entered)

UNCLASSIFIED

SECURITY CLASSIFICATION OF THIS PAGE(When Data Entered)

20. Abstract (Continued)

neon (0.6 torr) with an electron temperature in the same range. The corresponding classical resistance of the pinch is $9\text{m}\Omega$ whereas $500\text{m}\Omega$ is more consistent with output voltage pulse and current flow at interruption indicating anomalous resistivity is present. A one-dimensional two-fluid computer code has been developed to model anomalous resistivity in the pinch phase and preliminary results are consistent with the snowplow model. The final analysis of the plasma focus particle beam generation experiments was completed and a strong correlation was found for the beam-target model as the mechanism for neutron production in the Illinois plasma focus device.

11

UNCLASSIFIED

SECURITY CLASSIFICATION OF THIS PAGE(When Data Entered)

Abstract

Through collaboration with Dr. K. H. Schoenbach of Texas Tech University the plasma focus opening switch (PFOS) was revised to answer basic questions as to the utility of the concept. To estimate the plasma temperature and classical resistivity a soft X-ray spectrometer and X-ray pinhole camera were developed. The temperature was estimated from a coronal model to range between 0.4 to 0.5 keV for either a nitrogen or neon impurity (1 to 2%) in deuterium at 3 torr. Strong pinches were observed in pure neon (0.6 torr) with an electron temperature in the same range. The corresponding classical resistance of the pinch is $9\text{m}\Omega$ whereas $500\text{m}\Omega$ is more consistent with output voltage pulse and current flow at interruption indicating anomalous resistivity is present. A one-dimensional two-fluid computer code has been developed to model anomalous resistivity in the pinch phase and preliminary results are consistent with the snowplow model. The final analysis of the plasma focus particle beam generation experiments was completed and a strong correlation was found for the beam-target model as the mechanism for neutron production in the Illinois plasma focus device.

b) Research Objectives 1981-82

As indicated on the milestone chart for the 1981-82 proposal (Figure 1) the major research tasks were the development of

- 1) Soft X-ray diagnostics
- 2) Laser-interferometer for density measurements
- 3) Computer modeling of the plasma focus
- 4) High-Z gas operation of the plasma focus.

Due to budget limitations only the first item was completed and the rest are in various stages of development. Even to achieve this stage, equipment and computer time contributed by other funding sources had to be utilized. Also collaboration with Prof. K. Schoenbach from Texas Tech University (TTU) caused the direction of the research to be modified. This change emphasized the measurement of the plasma resistance for which the soft X-ray diagnostics are the most crucial. Thus all things considered good progress was made which will pave the way for completing the revised goals (as shown in Figure 2 for FY 1982-83) in a timely manner.

c) Status of Plasma Focus Opening Switch Research

- 1) Overview: collaboration with Prof. K. H. Schoenbach of Texas Tech University

After meeting Prof. Schoenbach at the 3rd Pulsed Power Conference in Albuquerque, NM in June 1981 and after having had several telephone conversations with him since that meeting it was realized that the possibility of fruitful collaboration existed. This was strongly encouraged by the grant monitor at that time, Lt. Col. A. K. Hyder, so in January 1982, G. Gerdin (principal investigator on this grant) traveled to Texas Tech University for a three day visit to discuss the possible nature of this collaboration.

Prof. Schoenbach is an ideal man with whom to collaborate since he had been involved with dense plasma focus (DPF) research for about ten years and is the author of over ten papers on the subject. Presently he is directing a project on diffuse discharge opening switches and so has experience in both DPF and opening switch physics.

A previous unsuccessful attempt to use the plasma focus as an opening switch¹ was regarded as not a true test of a plasma focus as an opening switch (see Appendix A). That is, it did not appear the device had been operated in an optimum manner since no capacitive discharge data showing strong interruptions were presented² and the initial \dot{I}_0 was very low.² Furthermore the circuit used² represented a brute force approach and the results indicated a more sophisticated circuit or gas handling technique would be required (see Appendix A). So a research program was devised to provide experimental tests to gain an understanding of the DPF interruption physics under ideal conditions of a capacitive energy drive and static gas fill.

The research program will answer these four basic questions:

- a) Is the interruption (Figure 3) inductive (\dot{L}) or resistive in nature?
- b) Can the power be tapped into a load?
- c) Can the timing of the interruption be controlled?
- d) Can the operation be made repetitive?

The resulting program is discussed in detail in Appendix B and presented in Figure 2.

The work performed during 1981-82 will have the most impact on the first year of this plan. The main goal of the first year of this program is to measure the resistance of the plasma focus and compare it with classical resistivity. To determine the latter, experimental measurements of the electron temperature, the plasma charge state and shape are the most crucial.³ These parameters can be resolved by soft x-ray diagnostics and the nature and results of these measurements will be discussed in section C2.

The computational effort has centered about the development of 1-D two fluid MHD computer code to model the collapse (interruption) phase of the DPF and the status of these calculations will be discussed in section C3.

The final analysis of the beams generated by the plasma focus based on results reported last year will be presented in section C4.

C2: Soft X-ray Analysis of a Dense Plasma Focus

General Introduction and Purpose

An experiment to detect and analyze soft x-ray radiation coming from the pinch of the Illinois Dense Plasma Focus (DPF) has been designed, constructed and performed during the summer and fall semester 1982. The experiment was designed to determine the electron temperature of the D.P.F., an important parameter in most plasma calculations. The detection of the x rays is performed by silicon solid state devices (pin diodes) conveniently filtered by matched metal foils in an arrangement known as Ross-Filter Technique⁴⁻⁷. The analysis of the experimental data is handled through a computer model of the observed plasma to give the electron temperature as a function of an experimentally measured parameter: the ratio between the detected intensities of selected spectral bands⁶.

Hardware

The x-ray spectrometer (XRS) consists of a long (3.0 m) evacuated aiming tube with a tightly packed array of three pin-diodes at one end. An aluminized Mylar vacuum window at the other end, housed in a revolving ball valve, couples the XRS with the focus, allowing easy aiming of the spectrometer. The interface of the XRS with the DPF chamber is completed by an adapter flange which permits vertical movement of the spectrometer and by a bellows connection which allows horizontal movement. An extension pipe protrudes into the DPF chamber, as close as 2 inches away from the axis, allowing excellent space resolution. (Figure 4). The device is aimed through the combination of bellows, adapter flange and extension pipe and this operation is performed routinely by members of the DPF experimental group before each data run.

The spectrometer is kept under vacuum ($<5\mu$) by a sieve-trapped mechanical pump. This prevents the soft x rays from being significantly attenuated on their way to the detectors. The spectrometer is also electrically insulated from the DPF chamber (which rises to high potential during the capacitor bank discharge at the firing of the focus).

The solid state detectors used in the experiment are Quantrad 100-PIN-250 doubly-diffused silicon pin diodes (Figure 5). They were chosen because of their high sensitivity in the region of interest (0.1 to 10 keV) and fast rise time (~ 2 nsec.) which allow good resolution in both space and time⁷.

Each pin diode is filtered by a different metal foil. The effective thicknesses of the foils (thickness/sine of angle of inclination) are matched so that their attenuation power is the same for all three filters except in the regions between absorption k edges. (Figures 6,7,8). The metal foils used are

1. Beryllium ($1.1 \cdot 10^{-1} \text{g/cm}^2$; k edge at 0.11 keV)
2. Aluminum ($4.1 \cdot 10^{-3} \text{g/cm}^2$; k edge at ~ 1.5 keV)
3. Nickel ($4.9 \cdot 10^{-4} \text{g/cm}^2$; k edge at ~ 8 keV)

By subtracting the signal of pin diode one from that of two (2-1) and the signal of pin diode two from that of three (3-2) it is possible to obtain two values proportional to the intensity of the radiation emitted in the regions between k edges (0.1 to 1.5 keV, 1.5 to 8 keV). Pictures of the pin-diode signals are included. (Figures 9, 10).

This information is the experimental data that is compared to the curve generated by a computer simulation, according to a given theoretical model, to yield a value for the electron temperature. Future improvements of the detection system include the addition of two more semiconductor detectors, for a total of five pin diodes, thus defining four adjacent radiation bands.

In addition to the pin diode XRS, a pinhole camera was constructed and used to detect time integrated x-ray radiation from the focus. (Figure 4).

The pinhole camera is connected to the chamber port opposite to the x-ray spectrometer. A 1 mil thick beryllium window is used, with a 20 mil diameter tantalum pinhole. The camera is flushed with helium during operation, to minimize attenuation of x rays. No x-ray radiation could be detected without helium flushing, thus indicating the predominance of x rays from the soft region in the focus emission and/or the lack of film sensitivity to harder x rays.

Software

The computer simulation of the DPF plasma x-ray emission uses a steady state optically thin corona model approximation. This is consistent with previous studies on the subject.^{8,9} A code has been developed to calculate the x-ray emission from the focus and the frequency-integrated response of the filtered pin diodes as a function of electron temperature.¹⁰ The following input data are required:

1. Thickness of filter foils and absorbing power as a function of frequency (energy).
2. Composition of the pin diodes.

3. Cross sections for collisional ionization and radiative recombination.⁶
4. Probabilities of excitation and de-excitation for various states.¹¹
5. Information on line radiation emitted in the region of interest.

The code evaluates:

1. Charge state equilibrium conditions.
2. Continuum radiation (Bremstrahlung + recombination)^{12,13}
3. Line radiation (decay of excited states).
4. Response curve of filtered pin diodes.
5. Response of pin diodes to the x-ray radiation emitted by the plasma defined above.
6. Differences in magnitude between responses (band strengths) and ratios of band strengths.

The final output is a table of ratios of band strengths vs. electron temperature, to be compared with the experimentally observed ratios.

A steady state corona model is presently used in the code.^{5,8} A more sophisticated version of the corona model is now being considered for implementation, which uses more recent and accurate values of cross sections.^{6,14-16} Also a local thermodynamical equilibrium (LTE) model is going to be used to evaluate what differences, if any, the LTE assumption introduces in the determination of the plasma state and the electron temperature. Eventually a full radiation-collisional time dependent code will be used in conjunction with an MHD code to model the x-ray emission during the pinch phase of the plasma focus.¹⁶⁻¹⁸

Results

Preliminary results based on simple steady state corona model show good consistency, yielding temperature values of about 0.4 to 0.5 keV, regardless of the type of impurity gas present (neon vs. nitrogen). (Figure 11). This result is encouraging since most of the detected x-ray emission from nitrogen seeded plasma is of the continuum type, as opposed to a neon contaminated plasma, where the neon line radiation dominates the detected emission. Roughly the same temperatures are expected in both cases, given the small amount of impurity gas present (about 2%). (Figure 11). Strong pinches were observed with pure neon as the working gas (0.6 torr) and with temperatures about the same as reported above.

Copper line radiation from the center electrode (hollow) has been determined to be negligible, on account of the following results:

1. X-ray emission increases by a factor greater than 10 when impurities (neon or nitrogen) are present. Almost no signal is detected by the filtered pin diodes for pure deuterium fills.
2. X-ray pinhole camera pictures show x-ray emission mostly from the pinch region. (Figure 12). Compare with Ref. 4 (solid center electrode).

The time integrated pictures of the x-ray emission from the focus also indicates an upper limit of 1-2 mm for the diameter of the pinch. When the absolute response of the pin diodes (supplied by the manufacturer) is used, together with the nominal solid angle of view, the measured size of the pinch, and the actual signal observed, the electron density can be estimated. The values of the electron density calculated in this way are between $6 \cdot 10^{18}$ and $3 \cdot 10^{19}$ electrons/cm³ for an optically thin plasma.

A simple check of this estimate can be made assuming magnetic to thermal pressure balance ($\beta=1$) and using experimentally evaluated parameters (pinch current = 300 kA, pinch radius = 0.5-1 mm, electron temperature = 500 eV). This yields values for the electron density in the same range ($8 \cdot 10^{18}$ to $5 \cdot 10^{19}$ electrons/cm³) depending on assumptions for the ion temperature ($T_i=0$ or $T_i=T_e$) and plasma radius. These values are consistent with measurements of plasma focus densities using laser interferometric,¹⁹ and laser scattering²⁰ techniques on devices of similar energy. This fact supports the validity of the model used in evaluating the experimental data and specifically of two assumptions that have been made:

1. Line radiation from other impurities (such as electrode material) is not important (the model ignores it).
2. Self absorption of radiation by the plasma is negligible (the model uses the optically thin approximation).

Also it is possible to calculate the classical (Spitzer) resistance of the pinch from the evaluated dimension of the x-ray image of the pinch. This is roughly 9 m Ω at a temperature of 500 eV. This value is about fifty times lower than the observed 0.5 Ω value (from current interruption measurements) suggesting the possibility of non-classical (anomalous) resistivity playing an important role in the focus current interruption at pinch time.

Conclusions

A combination x-ray spectrometer and pinhole camera has been built and tested. X-ray spectral analysis of radiation from the Illinois dense plasma focus has been performed to determine the electron temperature of the pinching plasma. Preliminary results indicate a temperature in the range

of 400 to 500 eV. These results are supported by cross checks on electron density calculations. Improvements have been planned and are being implemented in both the experimental hardware and software.

C3: Theoretical and Computational Effort

Although the research is primarily an experimental study, about one third of the effort is directed toward developing models for the plasma focus opening switch behavior in circuits with realistic loads to obtain an understanding of the coupling of the circuit and plasma. Specifically the role of fluctuations in creating anomalous resistivity at pinch time appear particularly relevant. The results of the development of theoretical models will be compared with experimental results on a frequent basis to suggest further experimental tests and new ways toward achieving a repetitive opening switch.

Two computer codes have been developed. The first is a zero-dimensional circuit-dynamical model where the macroscopic radial motion of the plasma is predicted self consistently using the snow plow model, the Leontovich-Osovet's equation, and the circuit equation.²¹ Classical resistivity²² has been included in the model and the results will be compared with measured circuit parameters to try to determine the role of sheath motion (L^*). This code has been used to predict the magnitude of the voltage pulses. These are arising from sheath motion and they are found to increase with magnitude of current flow at interruption²³ in the same manner and magnitude as observed experimentally.²⁴

To do a more detailed check on the theoretical possibility of anomalous resistivity in a plasma like the plasma focus, a one dimensional (cylindrical geometry) computer model (DPFR) of the DPF has been written²⁴ in order to compare experimental results with theoretical anomalous transport

coefficients for various microinstabilities.²⁵ The equations are integrated using the Lax-Wendroff-Richtmeyer finite difference scheme²⁶ with the help of flux-corrected transport.²⁷ This approach has been successfully used in modeling theta pinch experiments²⁸ has been adapted to DPF geometry. The code calculates the density, temperature and axial electric field in the DPF as a function of time and includes the circuit equation self consistently. (Figure 13).

Previous DPF models^{29,30} have been based on pure MHD equations which cannot include the effects of turbulence, such as anomalous resistivity, and therefore, are unable to accurately predict the characteristics of DPF impedance.

For an initial pinch current of 450 kA with the ion acoustic instability included, the code predicts a peak plasma density of $3.0 \times 10^{19} \text{ cm}^{-3}$, peak electron temperature of 1.9 keV, $dI_{MB}/dt = -2.2 \times 10^{12} \text{ amps/sec}$ (where I_{MB} is the main bank current) and a peak resistivity of about 1000 X Spitzer. (The experimentally observed value of dI_{MB}/dt during the radial collapse is about $-1.9 \times 10^{12} \text{ amp/sec}$; see Figure 3.) Calculated profiles of the density, electron temperature, ion temperature, and the magnetic field are shown in Figure 14 at about one nanosecond before the electrons run away.

The code predicts the collapse time, t_c , (at constant fill pressure) to be inversely proportional to the initial current, I_0 , (see Figure 15) as consistent with the snowplow model³¹. The short collapse times are due to the initial density distributions (Figure 16) which were selected to match boundary conditions and shorten the computation time. More realistic initial density profiles will be run in the near future. The high ratio of T_e/T_i shown in Figure 14 are due to the lack of the effects of viscosity in the code

at present. The addition of classical³¹ viscosity into the code is part of the present effort. Thus the computational effort is off to a good start.

C4: Summary of Particle Beam Scaling Measurements

The results reported in the last annual report^{32,33} have implications on two aspects of DPF phenomena:

1. the neutron production mechanism, and
2. the acceleration mechanism.

These aspects will be treated in this section.

Since the total number of particles accelerated and their energy spectra have been determined one can use this information to predict the magnitude and the scaling of the axial beam target neutron yield with I_{MB} if a few simple assumptions are made about the target. If the target is assumed to be the cold gas ahead of the beam then it is independent of bank parameters. Similarly, if one assumes that a hot target (plasma) of density and length independent of I_{MB} , which is roughly consistent with several experiments.^{19,20,34-36} Even slowing down of the deuterons could be neglected for $T_e > 500$ eV for targets less than 10 cm in length. Thus in calculating the axial beam target neutron yield the following assumptions have been made:

1. The ion beam energy spectrum has the same power law dependence as the electron beam energy spectrum for a given I_{MB} .
2. $N_+/N_e = (M_+/M_e)^{1/2}$.
3. The ion and electron energy beam spectra are the same at all angles to the axis where the beams exist.
4. The target parameters are independent of I_{MB} .

5. The slowing down in the cold gas target is that for deuterons in 3 torr D_2 gas.³⁷
6. The slowing down in the hot plasma target is negligible.

The predictions of this model are compared with the experimental data in Table I.

Table I			
Phenomena	Experiment	Cold Target	Hot Target
$Y_n \propto I_{MB}^x, x$	4.6 ± 0.3	5.2 ± 1.0	4.8 ± 1.0
Target thickness		15 cm @ 3 torr	$2.9 \times 10^{18} \frac{\text{deuteron}}{\text{cm}^2}$
Y_n at 12.5 kJ	3.8×10^9	2.4×10^9	3.1×10^9
Anisotropy ($Y_{n0^\circ}/Y_{n90^\circ}$)	1.7 ± 0.2	2.2	1.7
Neutron pulse width at 3.2 meters	90 ns	+60 ns	+30 ns

+Assumes axial beam motion only and includes 20 ns pulse width.

The scaling and magnitude of the beam target neutron yield is consistent with either target model (Figure 17) and the electron beam scaling parameters reported previously^{32,33}. However, neither target model is adequate to explain the neutron pulse width. The long pulse width observed experimentally could be due to trapping of part of the beam in some magnetic structure of the focus as evidenced by the high ratio of DT neutrons to DD neutrons observed in other DPF experiments.^{34,38} Description of such trapping is beyond the scope of these target models. The observed anisotropy is consistent with only the hot target model.

Due to the assumptions made in the calculations, the agreement in the magnitude and scaling of the beam target model prediction of neutron yield and the experimental result only means that the axial beam target model cannot be ruled out. Probably the most questionable assumption is that the deuteron beam energy spectrum is the same at all angles (to 15°) with respect to the device axis. This is apparently true for the electron beam which is not always on axis (presumably due to the frozen hose instability³⁹) and yet always gives the same power law spectrum (within the error). The large uniform patterns of tracks observed in the SSNTD converter layer technique⁴⁰ (which has a lower energy threshold of about 150 keV) over a 19° angle with respect to the axis also supports the assumption. And finally, the deuteron energy spectra are roughly independent of angle for a 28 kJ DPF at 5 torr D₂ in the energy range from 0.9 to 4.5 MeV.³⁶

Acceleration Mechanism

It is clear from Figures 14 and 15 of ref. 33 that the electron (and hence ion beam) occur at the peak in \dot{I}_{MB} indicating that current interruption plays a role in the acceleration process. However, estimates of the induced voltage across the pinch from the observed voltage surge across the parallel plate transmission lines between the capacitor banks and the DPF device and $L\dot{I}$ (where L is estimated from pinhole camera pictures) indicate that only about 100 kV appears across the pinch due to \dot{I}_{MB} phenomena. This voltage is much too low to explain the high particle energies observed by simple diode acceleration if current interruption (\dot{I}) was the only source of the applied potential.

It has been suggested⁴¹ that motion of the current sheath could cause induced voltages much higher than $\dot{L}I$ effects and the computational results of Kondoh and Hirano²¹ contain estimates of the magnitude of this effect. The system of equations used by the latter authors has been programmed and used to estimate the induced voltage for the Illinois DPF device. The final radial collapse ($r_0 = 2.5$ cm) was modeled and the initial conditions were determined experimentally by placing a coaxial short across the open end of the plasma focus electrode and measuring the circuit characteristics when the device was evacuated. At 3 torr D_2 pressure, the code estimates total induced voltages range up to ~ 100 kV for a peak device current of 560 kA. Hence it appears that even sheath motion cannot provide sufficient potentials to explain the observed particle energies (which apparently range above 1 MeV in this device⁴⁰) by the simple process of diode acceleration.

Conclusions

The energy spectra of the fast ions and electrons emitted by the plasma focus in opposite directions (Figure 1 of ref. 33) are observed by direct methods to have the same power law energy dependence at a device current at pinch time, I_{MB} , of 560 kA. The scaling of the absolute value of the exponent of the power law was found (for electrons) to decrease with increasing I_{MB} (hardening of the spectrum) and the values found to be consistent with the electron energy spectra inferred from hard X-ray spectral measurements on several other devices.⁴²⁻⁴⁵ It is interesting that power law spectra of similar exponents have also been observed in a double inverse pinch,⁴⁶ cosmic rays,⁴⁷ and solar flares.⁴⁸

The magnitude of the fast electron current has been measured by a filtered fast Faraday cup and found to scale as I_{MB} to the third power. The highest primary beam current observed was 17 kA for a bank energy of 12.5 kJ. Since much more energetic plasma foci exist such as the 1MJ device at Frascati,³⁴ it would be very interesting if similar measurements were performed on these devices to see if the scaling observed in the Illinois device persists at high bank energy. If so, the hardening of the energy spectra indicated by these measurements and others⁴²⁻⁴⁵ may lead to new applications of the DPF as a pulsed electron beam source.

The measured beam parameters and scaling laws can be used to predict the scaling and magnitude of the neutron yield due to a beam target model. If the target parameters are assumed to be independent of I_{MB} , then the agreement between beam target yield and the observed yield is quite good with respect to scaling and magnitude but the predictions of the model do not fit the observed temporal neutron pulse width. It is possible that trapping of all or part of the deuteron beam by magnetic structures in the plasma focus³⁴ could explain the discrepancy.

The beams are observed to occur at the peak in the current interruption (\dot{I}_{MB}) indicating the latter has a strong influence on the acceleration process but the magnitudes of the voltages generated by d/dt (LI) effects estimated from circuit measurements are too low to explain the acceleration process by simple diode acceleration.

Since the beams are generated during the power pulse at the location of the current interruption the acceleration mechanism is likely to be fundamentally connected to the mechanism of current interruption. From the data presented here plasma diode acceleration formed by a plasma filled opening switch (current interruption) remains a strong candidate as the accelerating mechanism and hence voltage pulses of up to 1MV appear to be generated in the switch.

References

1. J. Salge, "Problems of Repetitive Opening Switches Demonstrated on Repetitive Operation of a Dense Plasma Focus," Workshop on Repetitive Opening Switches, M. Kristiansen and K.H. Schoenbach ed., Texas Tech. U., Lubbock, TX 79409, 189 (1981).
2. J. Salge, U. Braunsberger, B. Fell, I. Ueno and H. Conrads, Nucl. Fusion 18, 972 (1978).
3. L. Spitzer, Jr. Physics of Fully Ionized Gases, 2nd Ed. (Interscience, New York, 1962) 143.
4. J. W. Mather, Meth. of Exp. Phys. 9B (Academic Press, 1971) 229-30.
5. T. F. Stratton, in Plasma Diagnostic Techniques (R. H. Huddleston, S. L. Leonard, Eds., Academic Press, New York) 359 (1965).
6. C. De Michelis, M. Mattioli, Nuclear Fusion, 21, 677 (1981).
7. D. J. Johnson, Rev. Sci. Instrum., 45 191 (1974).
8. R. W. P. McWhirter, in Plasma Diagnostic Techniques (R. H. Huddleston, S. L. Leonard, Eds., Academic Press, New York) 201 (1965).
9. E. H. Beckner, J. Appl. Phys., 37 4944 (1966).
10. M. L. Watkins, Phys. Rep. 37 111 (1978).
11. I. I. Sobelman, Atomic Spectra and Radiative Transitions, (Springer-Verlag, Berlin, 1979).
12. P. J. Brussaard, H. C. Van de Hulst, Rev. of Modern Physics, 34 507 (1962).
13. J. Greene, Astrophys. J., 130 693 (1959).
14. R. F. Reilman, S. T. Manson, Astrophys. J. Suppl. Ser., 40 815 (1979).
15. R. Mewe, J. Schriener, J. Silvester, Astronom. Astrophys., 87 55 (1980).
16. D. Salzmann, A. Krumbein, J. Appl. Phys., 49 3229 (1978).
17. R. W. P. McWhirter, Phys. Rep., 37 165 (1978).
18. J. Magill, J. Phys. D.: Appl. Phys., 10 2257 (1977).
19. A. Bernard, A. Coudeville, A. Jolas, J. Launspach, J. DeMascureau, Phys. of Fluids, 18 180 (1975).
20. M. J. Forrest, N. J. Peacock, Plasma Phys., 16 489 (1974).

21. Y. Kondoh and K. Hirano, Phys. Fluids 21, 1617 (1978).
22. L. Spitzer, Jr., Physics of Fully Ionized Gases, 2nd Ed. (Interscience, 1962) 27-28.
23. J. Mandrekas, private communication.
24. W. A. Stygar, Ph.D. Thesis, University of Illinois, Urbana-Champaign, (1982).
25. R. C. Davidson and N. A. Krall, Nuclear Fusion 17, 1313 (1977).
26. R. D. Richtmyer and K. W. Morton, Difference Methods For Initial Value Problems (Interscience, 1967).
27. D. L. Book, J. P. Boris and K. Hain, J. Comp. Phys. 18, 248 (1975).
28. P. C. Liewer and N. A. Krall, Phys. Fluids 16, 1953 (1973).
29. S. Maxon and J. Eddleman, Phys. Fluids 21, 1856 (1978).
30. D. E. Potter, Phys. Fluids 14, 1911 (1971).
31. S. I. Braginski, Rev. Plasma Phys. 1, 205 (1965).
32. G. Gerdin, Interim Annual Report 30 Sept. 1980-30 Sept. 1981, Fusion Studies Lab Report #FSL-68 Nov. 30, 1981.
33. W. Stygar, G. Gerdin, F. Venneri and J. Mandrekas, Nuclear Fusion, 22, 1161 (1982).
34. J. P. Rager, "Progress on Plasma Focus Research at Frascati," C.M.E.N. Report 81.43/cc C.N.E.N.-Edizioni Scientifiche C.P. 65 00044 Frascati Rome, Italy (Sept. 1981).
35. K. Hirano, K. Shimoda and F. Hamada, Jap. J. Appl. Phys. 17, 1619 (1978).
36. H. Schmidt, Atomkernenergie-Kerntechnik 36, 161 (1980).
37. H. H. Andersen and J. F. Ziegler, Hydrogen Stopping Power and Ranges in all Elements: Stopping and Ranges of Ions in Matter, 3 (Pergamon Press, New York, 1977).
38. K. Huebner, K. Steinmetz, J. P. Rager and B. V. Robouch, 1981 IEEE Int. Conf. on Plasma Sci. Conf. Rec.-Abstracts, IEEE Catalog No. 81 CH1640-2 NPS, 59 (1981).
39. S. Putnam, Transverse Instabilities of Intense, Relativistic Electron Beams, PIIR-7-68, Physics International Co., San Leandro, CA, March, 1968.
40. G. Gerdin, J. Durham and R. Illic, Nuclear Tracks 5, 299 (1981).

41. C. E. Newman and V. Petrosian, Phys. Fluids 18, 547 (1975).
42. J. H. Lee, D. S. Loebbaka and C. E. Roos, Plasma Phys. 13, 347 (1971).
43. R. L. Gullickson and R. H. Barlett, Adv. in X-ray Anal., 18, 184 (1971).
44. H. L. L. Van Paasen, R. H. Vandre and R. S. White, Phys. Fluids 13, 2606 (1970).
45. D. J. Johnson, J. Appl. Phys. 45, 1147 (1974).
46. P. J. Baum, A. Bratenahl and R. S. White, Phys. Fluids 16, 226 (1973).
47. B. Rossi, Cosmic Rays, (McGraw-Hill, New York, 1964), p. 174.
48. R. Ramaty, S. A. Colgate, G. A. Dulk, P. Hoyng, J. W. Knight, R. P. Lin, D. B. Melrose, R. Orrall, C. Paizis, P. R. Shapiro, D. F. Smith, and M. Van Hollebeke, "Energetic Particles in Solar Flares", in Solar Flares, P. A. Sturrock, Ed., (Colorado Assoc. Univ. Press, Boulder, CO, 1980), p. 117.

MILESTONE CHART

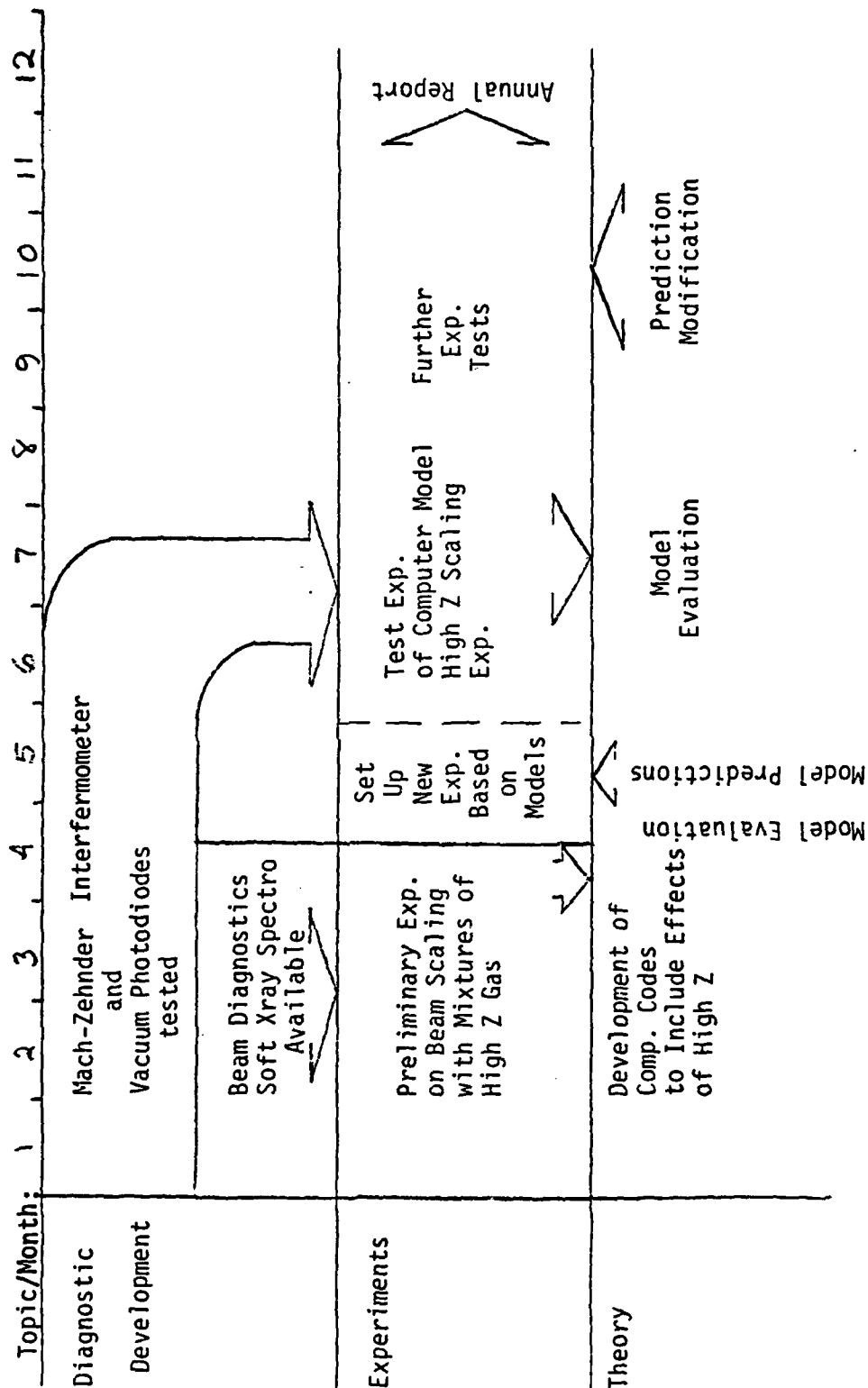
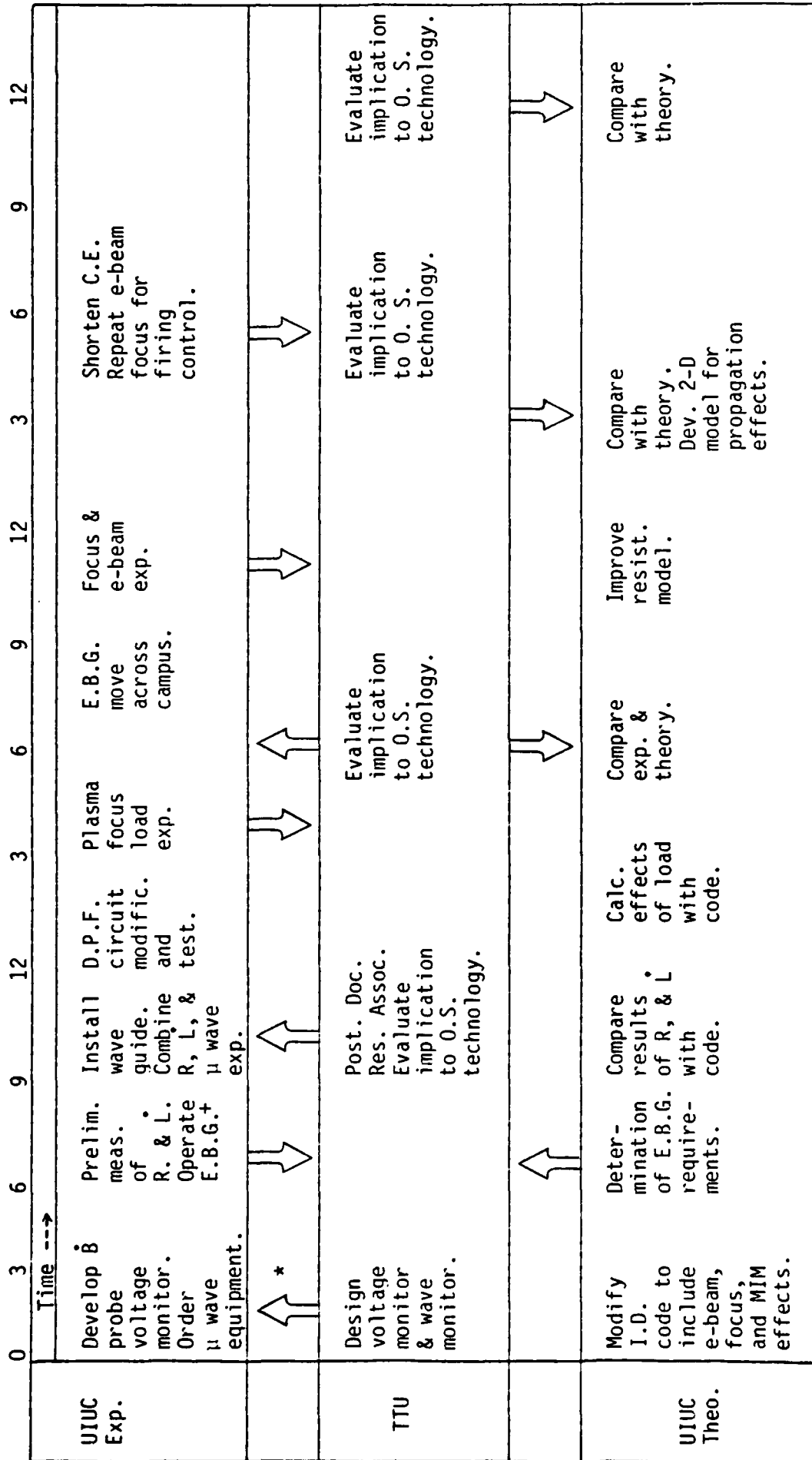


Figure 7 Milestone chart for the 1980-81 proposal.

Figure 2 Milestone Chart: Plasma Focus Opening Switch Experiments



+E.B.G. = Electron Beam Generator

*

➡ = Information flow

Figure 2 Milestone Chart: Plasma Focus Opening Switch Experiments

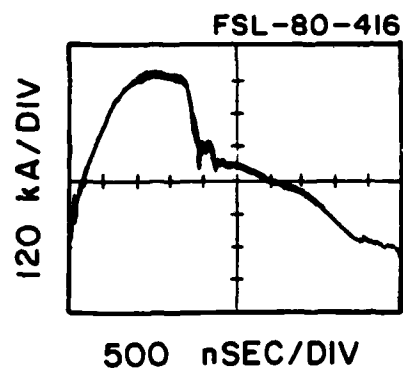


Figure 3 Wave form of the device current of the Illinois plasma focus as observed with a Rogowski coil.

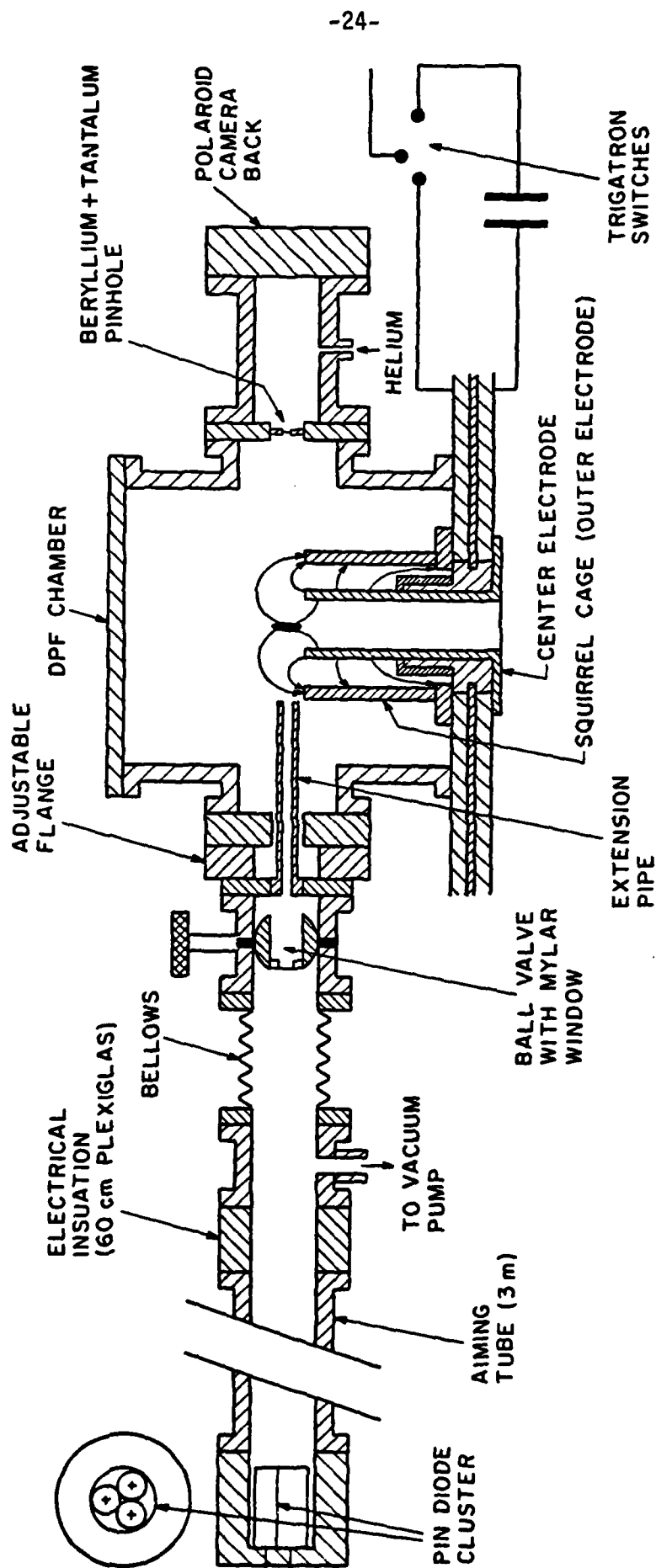


Figure 4 Experimental set-up, x-ray spectrometer on the left, dense plasma focus chamber, x-ray pinhole camera on the right. Total distance between x-ray pin diodes and focus = 4.5 m, diameter of extension pipe = 1.0 cm; sensitive area of detectors = 100 mm².

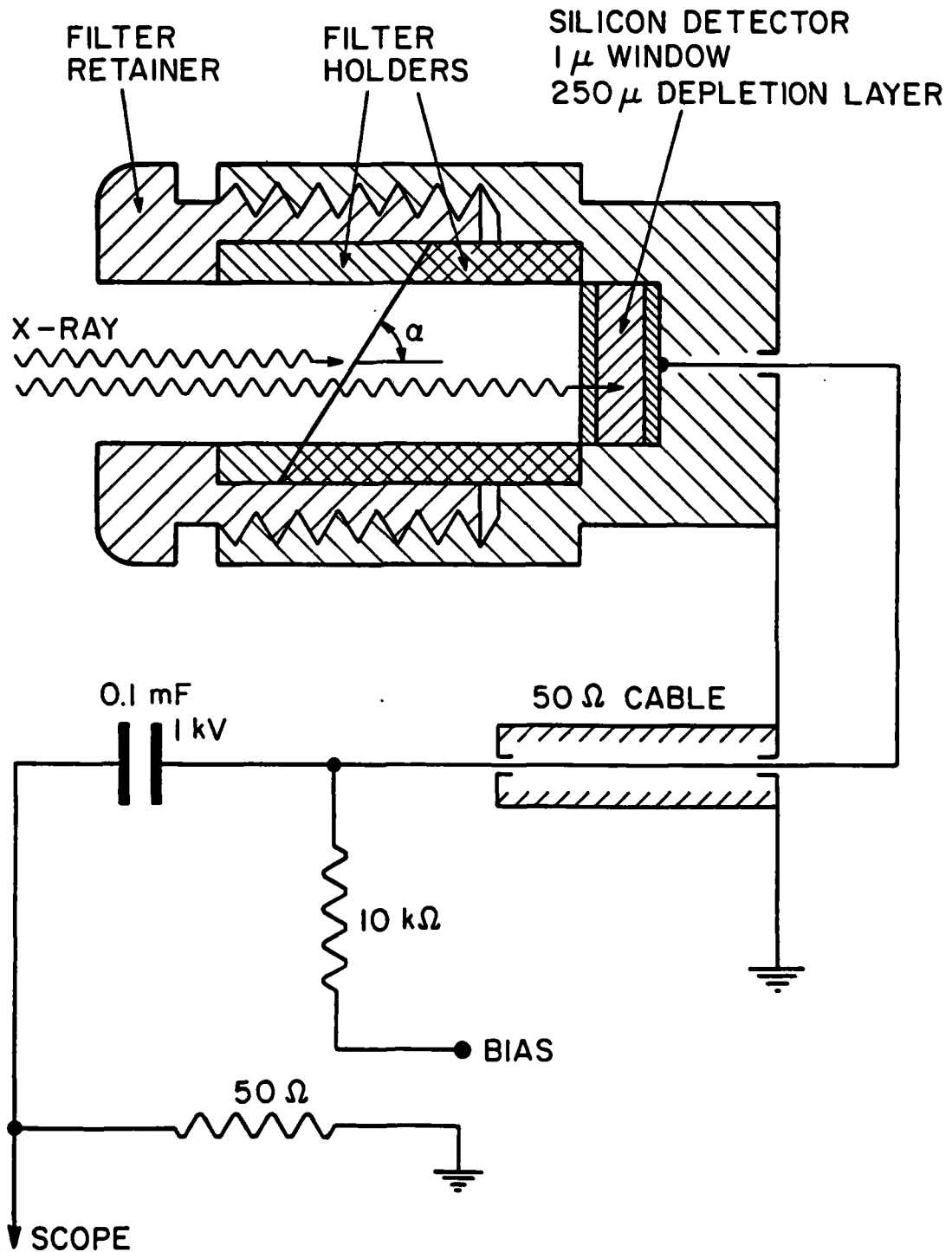


Figure 5 Schematics of pin diode detector circuit; pin diodes are Quantrad 100 PIN 250; bias voltage = -300 volts; α = angle of inclination of metal foils.

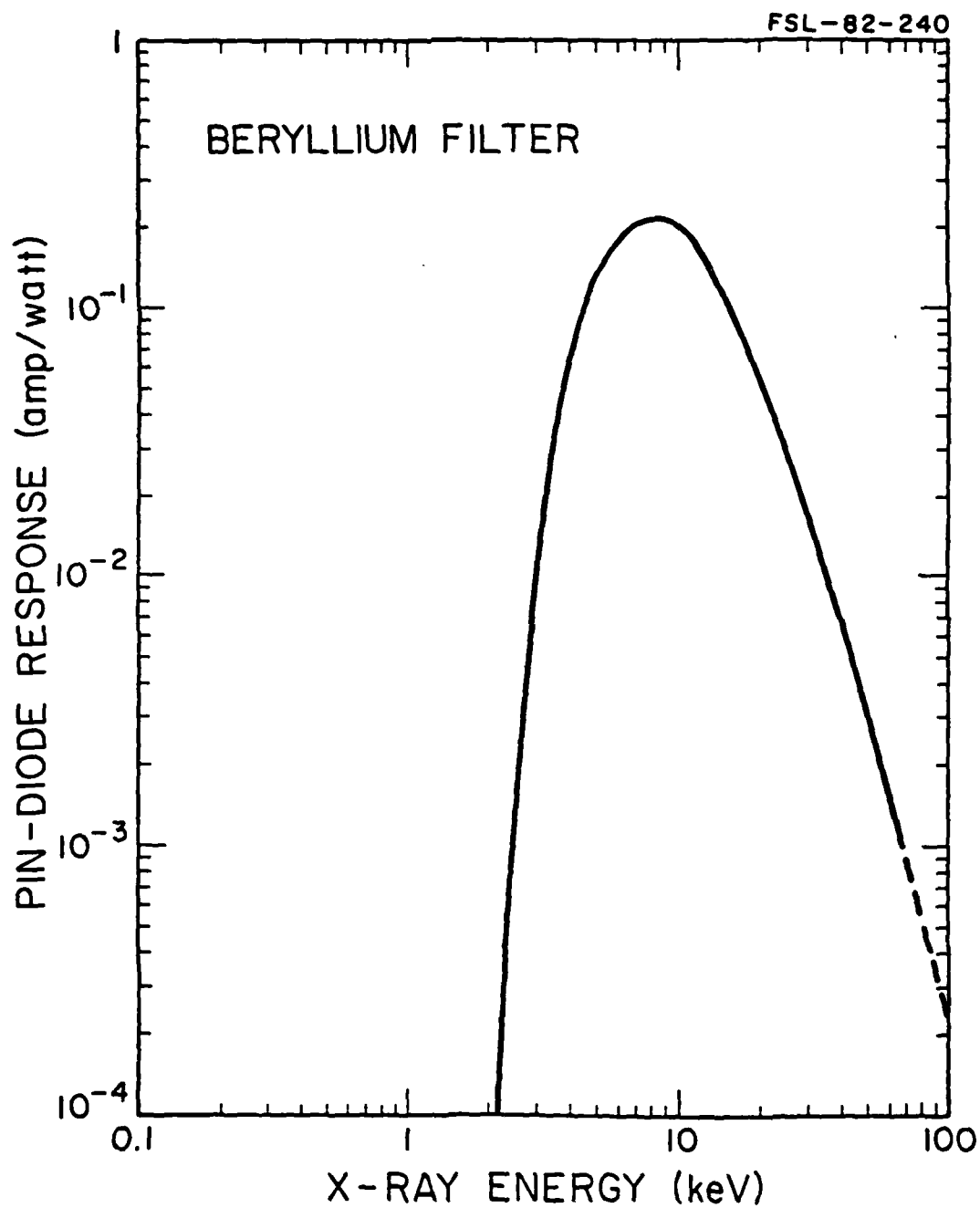


Figure 6 Pin diode response to x rays with beryllium filter
($1.1 \cdot 10^{-1}$ g/cm²) k edge at 0.11 keV.

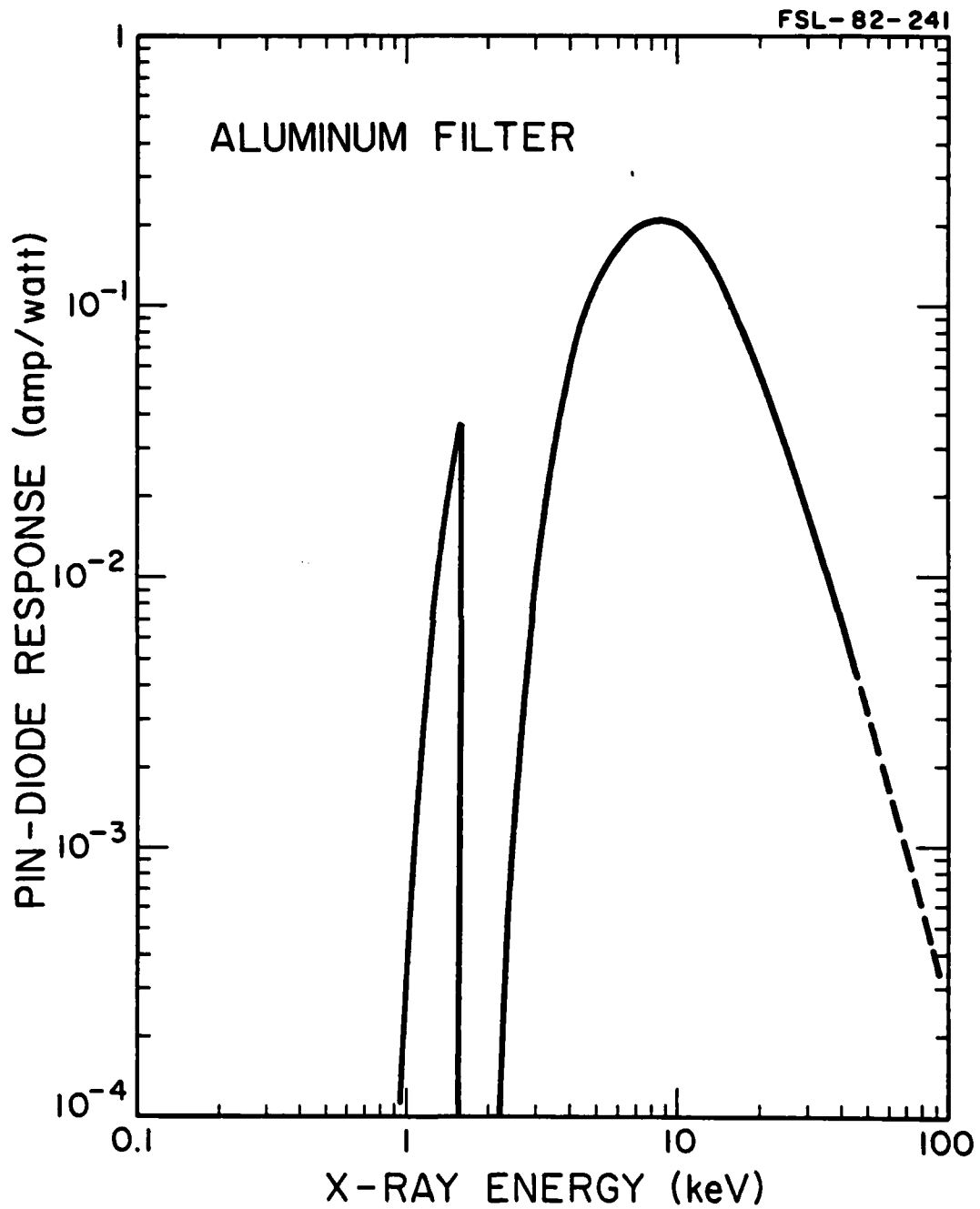


Figure 7 Pin diode response to x rays with aluminum filter
($4.1 \cdot 10^{-3}$ g/cm²) k edge at 1.56 keV.

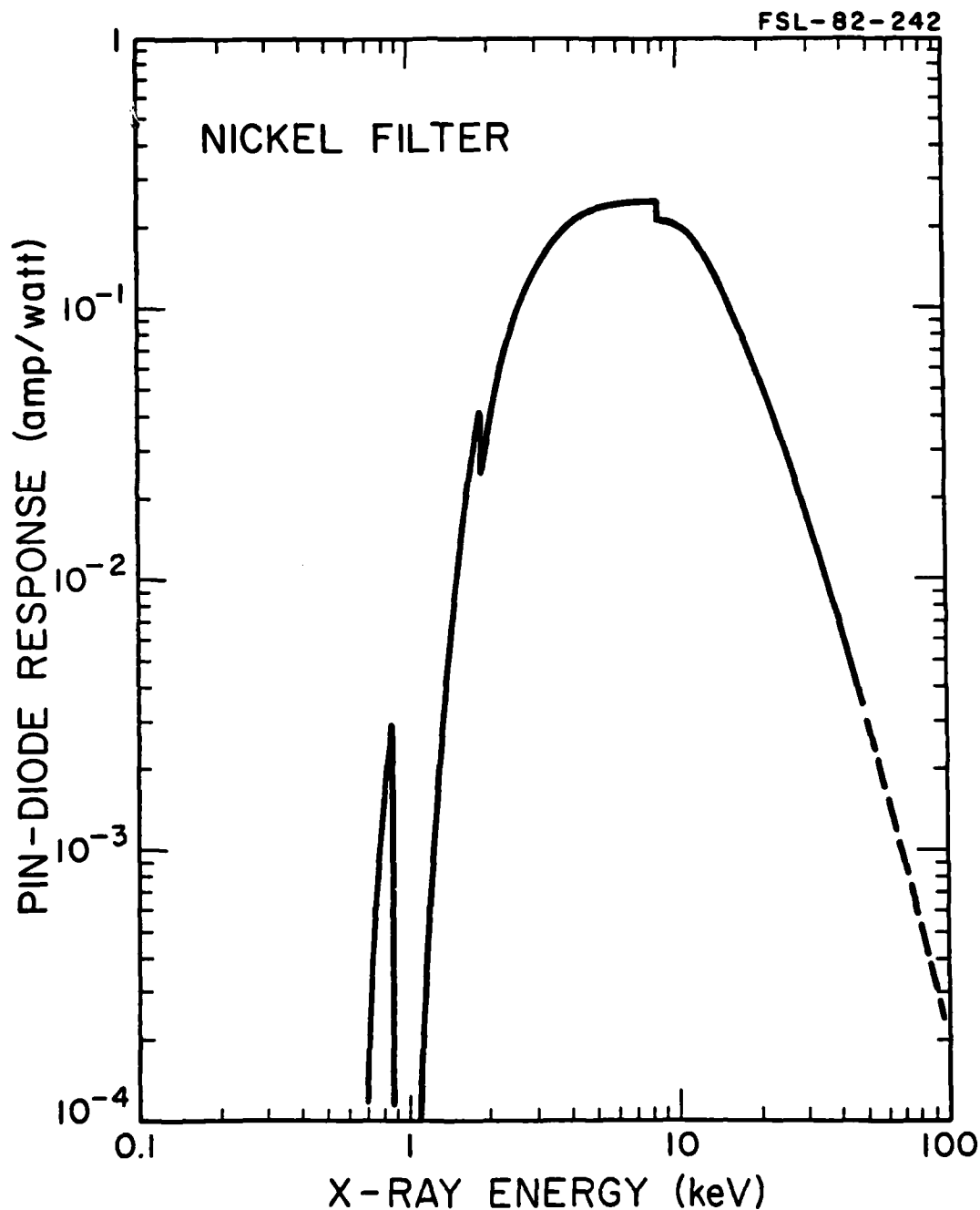


Figure 8 Pin diode response to x-rays with nickel filter ($4.9 \cdot 10^{-4}$ g/cm²), L-III edge at 0.862 keV, k edge at 8.33 keV silicon edge (pin diode) at 1.84 keV.

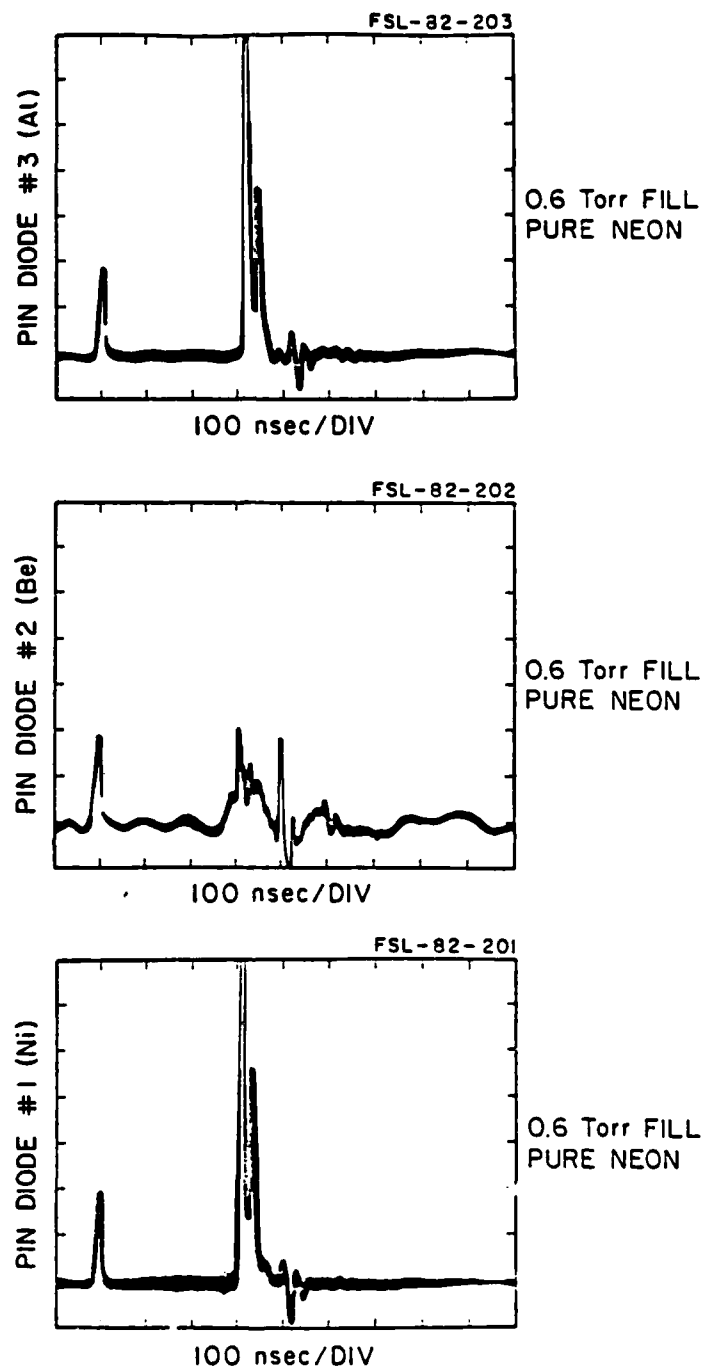


Figure 9 Filtered pin diode oscilloscope traces with 0.6 torr Neon as the fill gas.

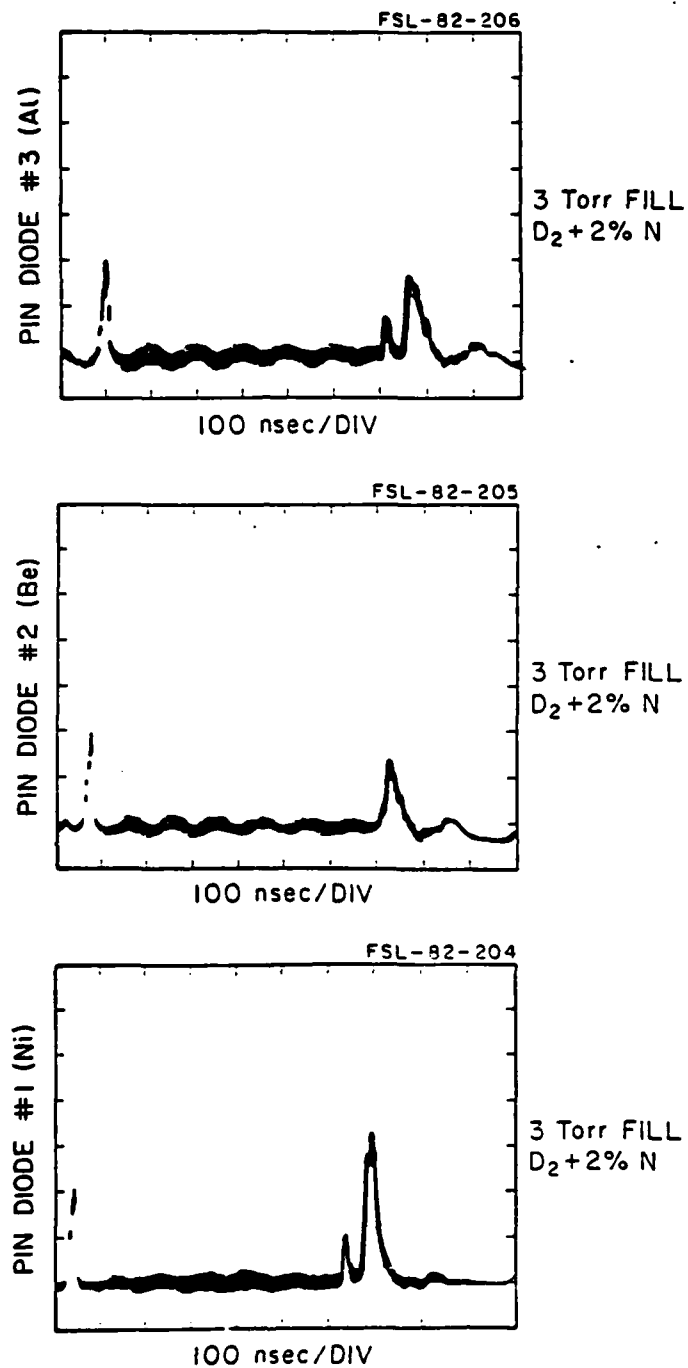


Figure 10 Filtered pin diode oscilloscope traces with 3 torr $D_2 + 2\%$ Nitrogen as the fill gas.

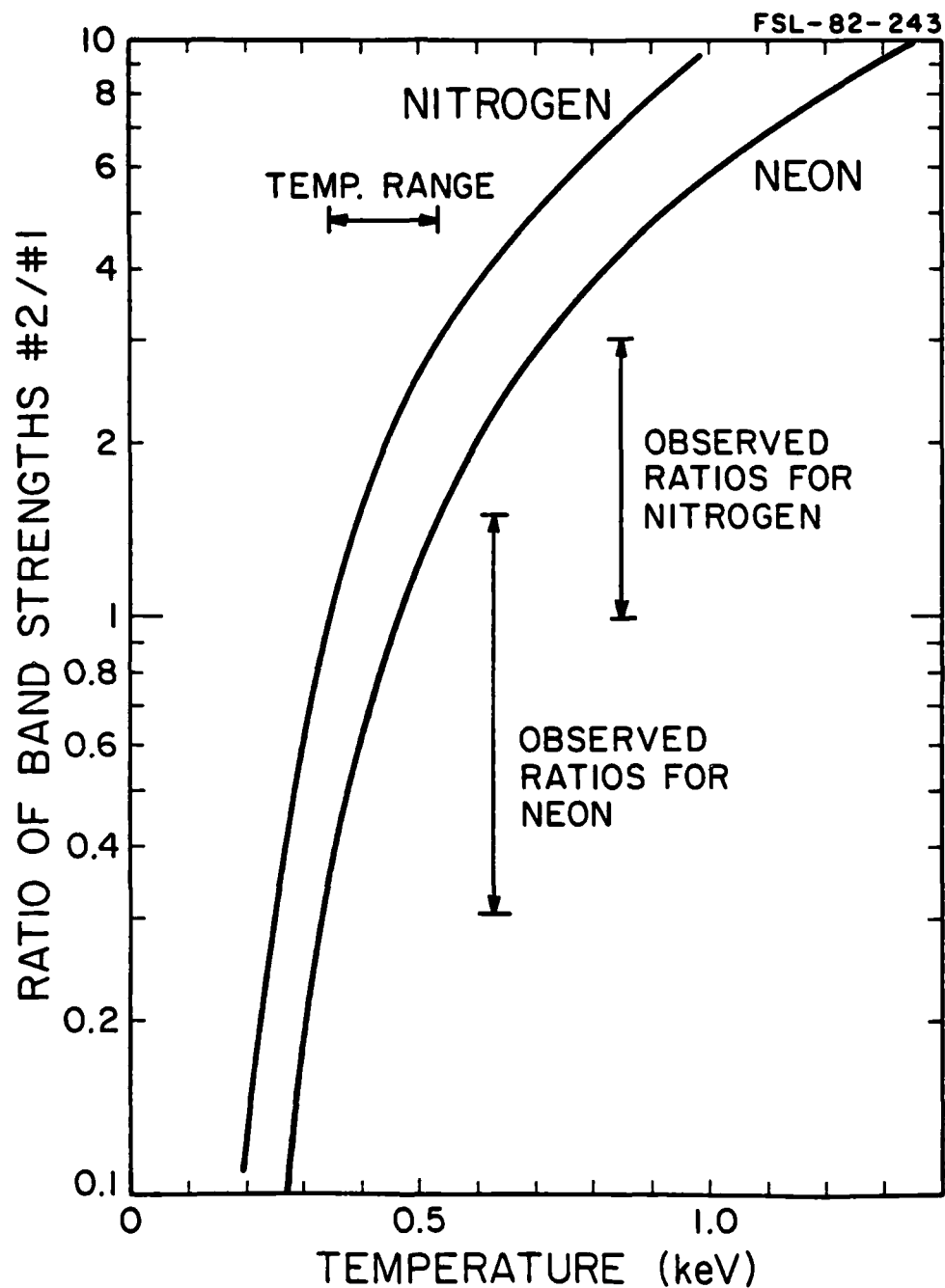


Figure 11 Ratio of band strengths vs. temperature, as determined by computer simulation (corona model) for deuterium fills with 2% nitrogen and 2% neon.

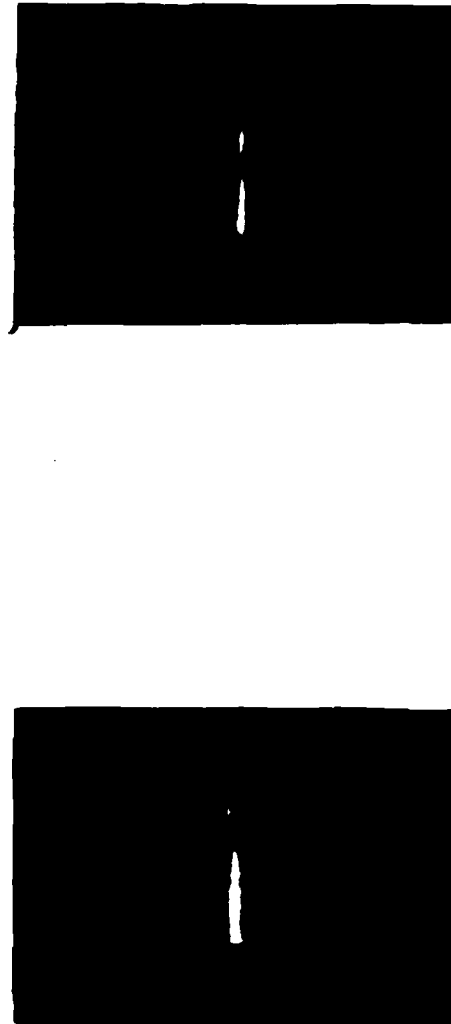


Figure 12 X-ray pinhole camera photographs of two separate shots of the DPF each resulting in a neutron yield of $2 \times 10^9 \pm 5\%$. The scale is 3/4 actual size.

FSL-81-130

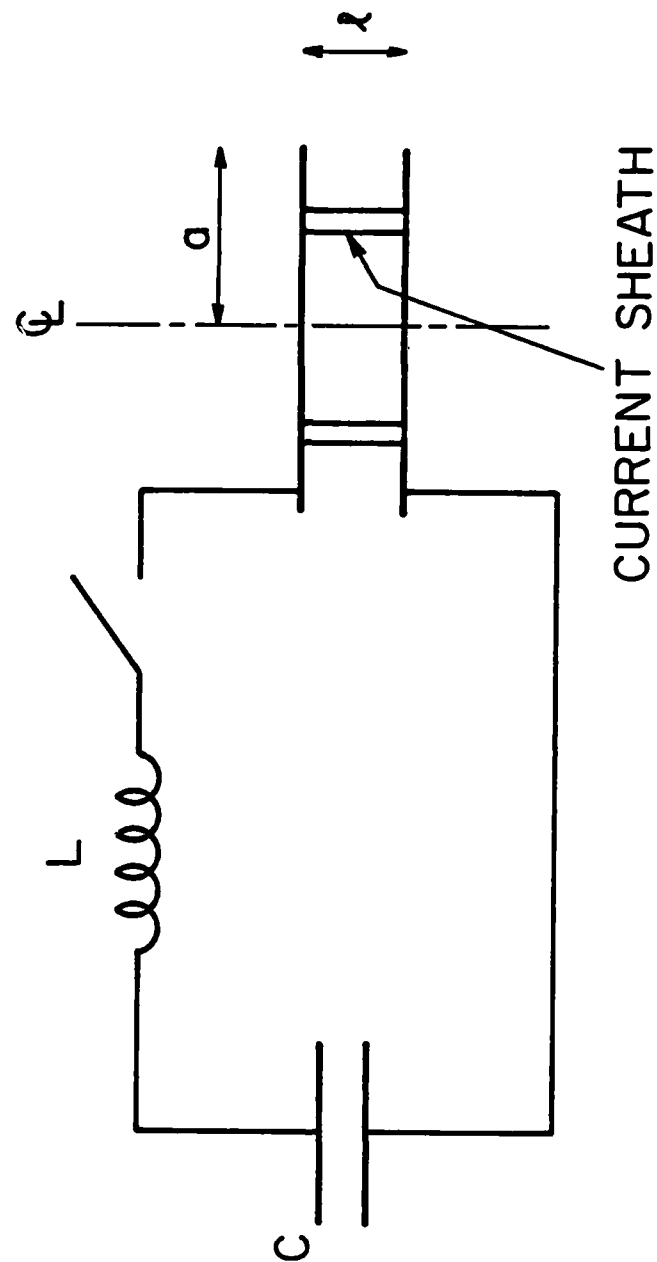


Figure 13 Idealized model of the DPF plasma-external circuit system.

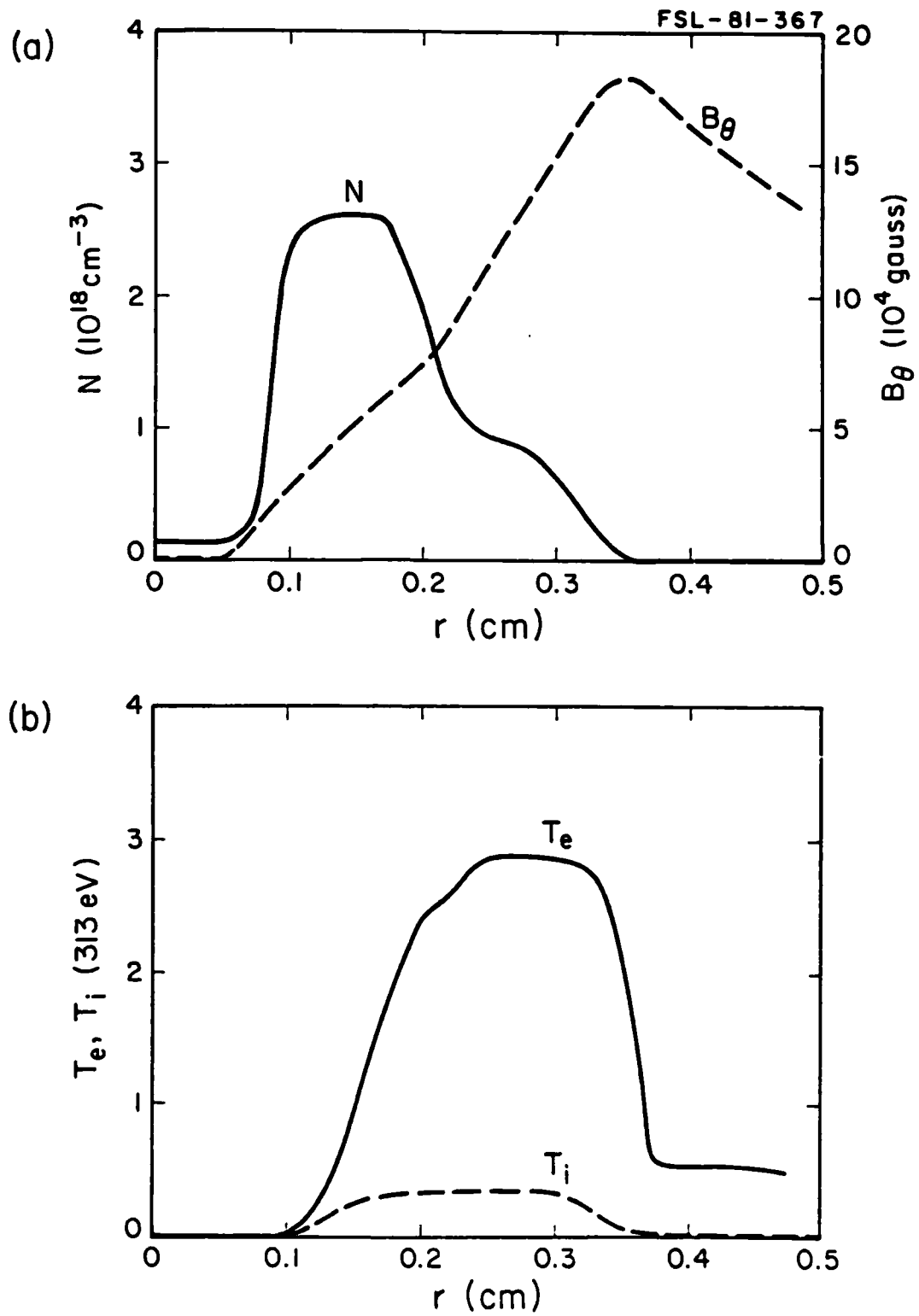


Figure 14 Density, magnetic field, electron temperature, and ion temperature profiles in the focus plasma about one nanosecond before the electrons runaway.

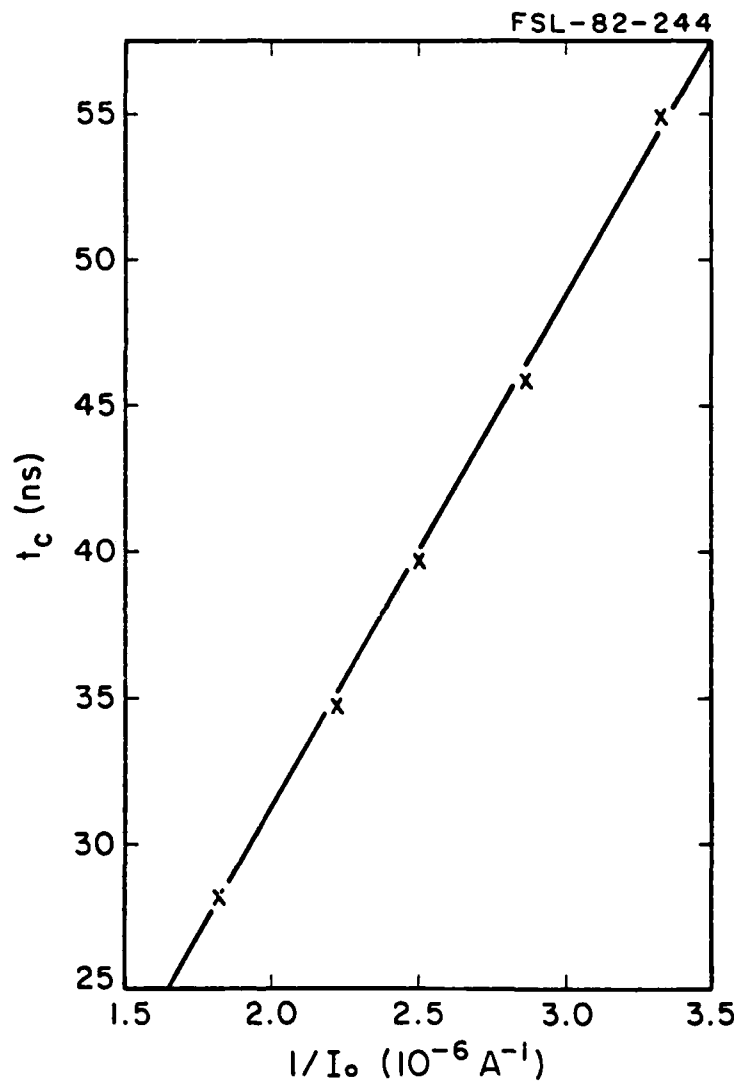


Figure 15 The dependence of radial collapse time t_c , on the inverse of the initial pinch current^c($1/I_0$), as computed by the one-dimensional two-fluid code. The snowplow model predicts these parameters ($1/I_0$, t_c) to be linearly related.

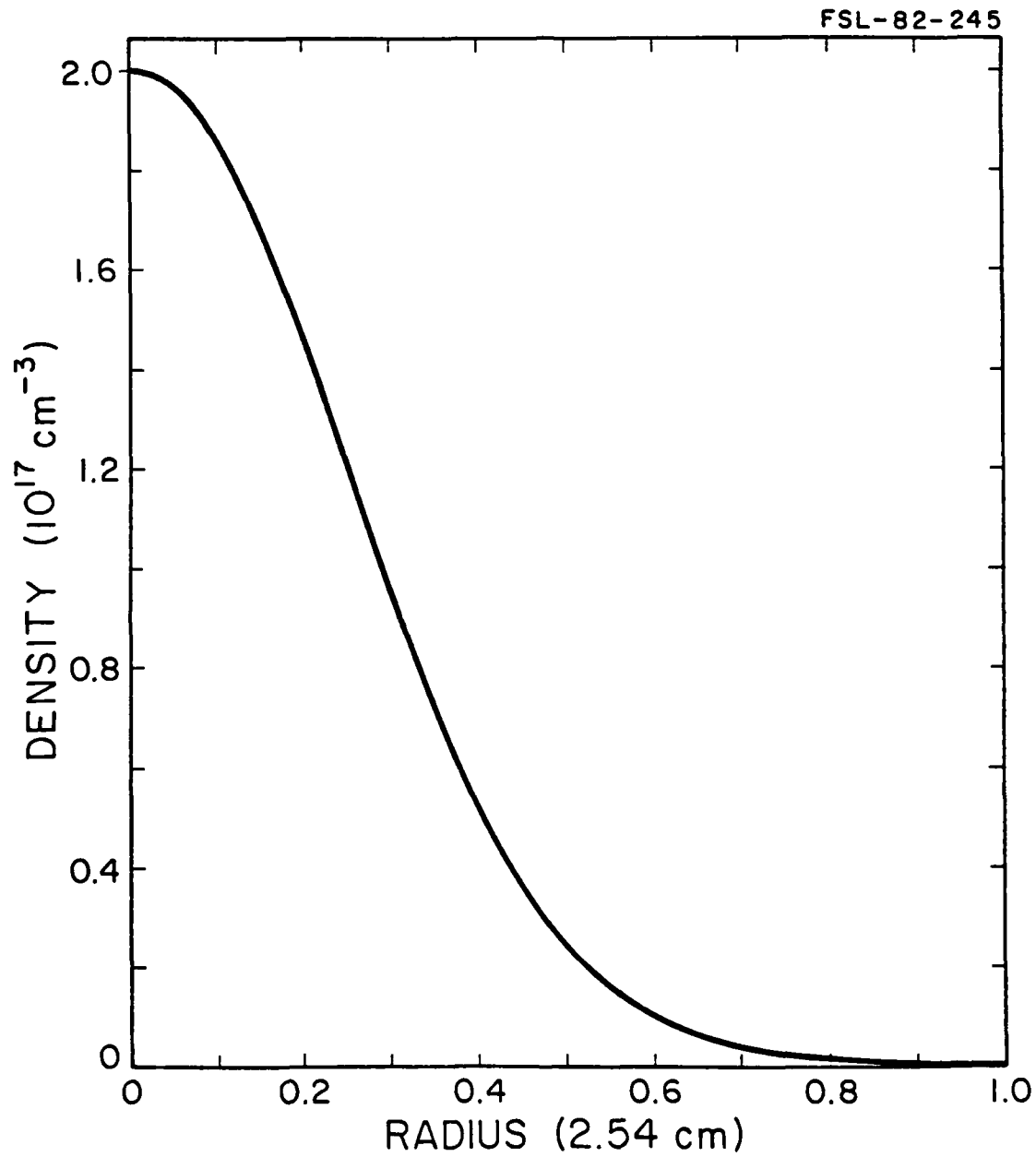


Figure 16 Initial density profile as used at present in the two fluid code.

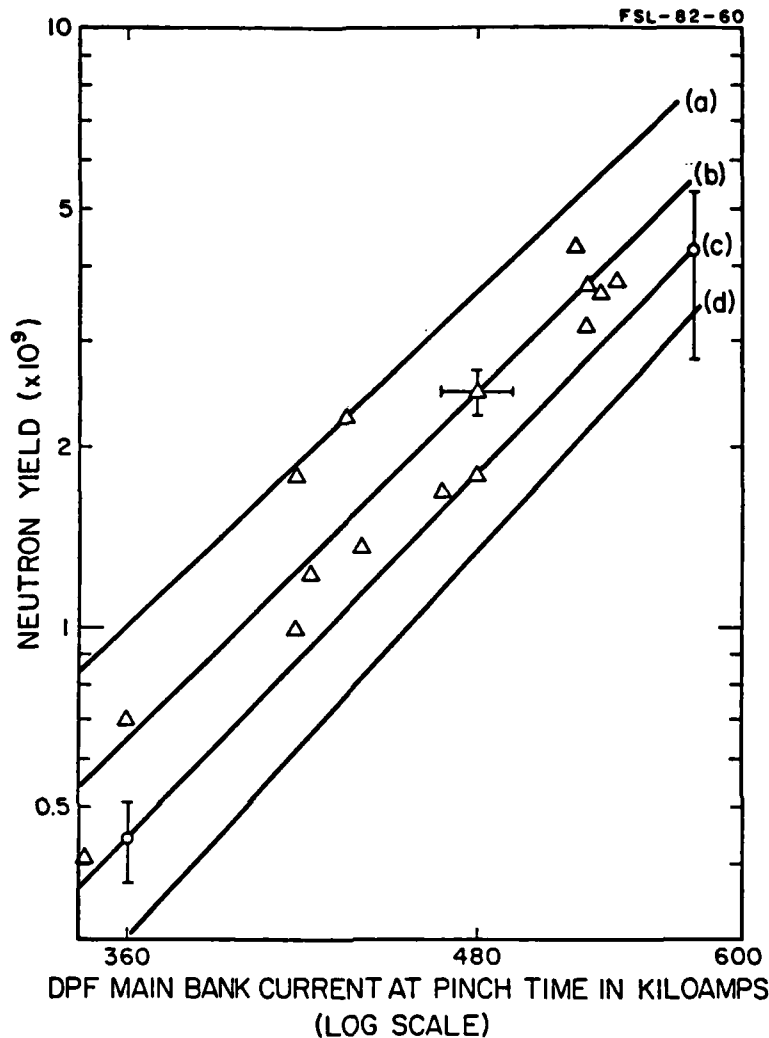


Figure 17 Neutron yield in the Illinois plasma focus and the predictions of various models.

- i) Curve a) is the least square fit to the peak neutron yield versus I_{MB} ($Y_n \propto I_{MB}^{4.4 \pm 0.3}$).
- ii) Curve b) is the least square fit to the neutron yield for the shots actually used to determine the electron-beam generation data. The triangles are the data with representative error bars shown for one of the points. For these data $Y_n \propto I_{MB}^{4.6 \pm 0.3}$.
- iii) Curve c) is the result of the beam hot target model for a target thickness of $2.9 \times 10^{18} \frac{\text{deuterons}}{\text{cm}^2}$.
The error bars are those associated with the experimental uncertainties in the beam parameters.
The model predicts $Y_n \propto I_{MB}^{4.8}$.
- iv) Curve d) is the result of the beam cold gas target for a target of 3 torr deuterium gas 15 cm long (target thickness $2.9 \times 10^{18} \frac{\text{deuterons}}{\text{cm}^2}$ as in iii) where the effects of slowing down on the deuteron beam have been included. The error bars are as in iii) and this latter model predicts $Y_n \propto I_{MB}^{5.2}$.

Appendix A: A previous opening switch experiment and its implications.

A previous opening switch experiment¹, where a DPF was utilized to interrupt the current stored in a large inductive coil (see Figure A1), was somewhat unsuccessful in the sense that the interruptions and power pulses generated were irregular and variable in magnitude.

The experiments were successful in that several focus interruptions occurred over a period of 150 μ sec (a factor of fifty longer than normal) and thus these results show that a long series of power pulses may be possible if only the moment of interruption could be controlled. Understanding the nature of the current interruption and hence possible means of achieving firing control are a central task to DPF-opening switch research. Some progress can be made toward this goal by analyzing the experiments of Dr. Salge in more detail.

On reviewing the results of Salge's experiments¹ three things stand out:

- 1) The voltage across the device is always a few kilovolts during the pulse.
- 2) The initial time derivative of the device current, \dot{I}_0 , (as inferred from Figure 6 of ref. 1) is low (only about $2 \cdot 10^{10}$ A/s).
- 3) No strong interruption occurs at the initial pinch time and the maximum interruption is only 20% of the current.

These three points will be discussed in the rest of the appendix.

The first point illustrates that the gas in the Salge DPF experiments was never given a chance to recover (recombine) and hence each successive pinch and interruption depends on the distribution of the ionized gas left by the previous one (see Figure 4 of ref. 1). Since the conventional DPF

even under ideal conditions is not very reproducible in shape (see Figure 12) it should not be too surprising that erratic behavior was present. Stabilizing the plasma with a small axial magnetic field as demonstrated by Mather^{A1} may be one promising approach to improve Salge's experiment and will certainly be tested in stage 4 of the proposed research schedule (during the third year, see Figure 2).

Another approach to firing control might be to allow the gas to completely recombine between shots. A plasma focus has been operated at a rate of 1 Hz for 150 shots.^{A2} Only two shots in this sequence had no neutron yield and the rest were within 50% of $5 \cdot 10^9$ neutrons/shot. Since strong neutron yield is associated with sharp current interruption this latter result is especially encouraging. The upper limit to the repetition rate in the gas recovery mode (besides being limited by the power supply) is the inverse of the deionization time. Since the operating pressures and gap dimensions are roughly those of a hydrogen thyratron^{A3}, the deionization time would be about 5 μ sec. Hence the fundamental limit on the rep. rate in this mode would be $\sim 10^5$ Hz.

Thus the high voltages occurring across the DPF during Salge's experiments and the resulting erratic behavior are neither surprising nor fatal to the DPF opening-switch concept although fairly sophisticated circuitry may be required for repetitive operation if the simple technique of magnetic stabilization^{A1} is unsuccessful. The gas-recovery-DPF mode circuitry is currently under study.

The last two points indicate that possibly little of the device current was carried by the pinch in Salge's experiment and hence the low percentage interruptions. Much stronger current interruptions and neutron yields have

been reported^{A4} for a device of similar size and carrying similar current which had an \dot{I}_0 of $4 \cdot 10^{11}$ A/s as opposed to $2 \cdot 10^{10}$ A/s in the Salge experiments^{1,2}. High-power DPF experiments driven by a magnetic flux compressor^{A5} (which has a similar problem of low \dot{I}_0 as does Salge's inductive energy store) have reported^{A6} that a minimum \dot{I}_0 is required for good focus performance and \dot{I}_0 minimum is dependent on filling pressure. This dependence ranges from $1.5 \cdot 10^{11}$ A/s to 10^{12} A/s for a filling pressure of 10 to 22 torr deuterium.

One might expect an effect of the \dot{I}_0 on performance since the time the focus discharge dwells in a given region depends on \dot{I}_0 . Long dwell time could cause that region to heat and hence cause gas to evolve from that region. If enough gas evolves behind the current sheath as it moves away (Figure A3) a second sheath may occur behind the first sheath and hence limit lowering the current in the subsequent pinch caused by the collapse of the first sheath. This behavior has been found to occur in plasma focus devices of relatively low \dot{I}_0 .^{A7}.

The time, t , for the current sheath to run to a given distance Z along the central electrode can be shown to be

$$t = \frac{Z^{1/2} \rho_0^{1/4}}{\dot{I}_0^{1/2}} \left[\frac{24\pi^2 (b^2 - a^2)}{\mu_0 \ln(b/a)} \right]^{1/4}$$

where ρ_0 is the mass density of the fill gas, and a and b are the radii of the inner and outer electrodes respectively. This formula yields the

dependences on ρ_0 and \dot{I}_0 observed in experiment^{A1} and gives order of magnitude results. It can be seen that the dwell time in the vicinity of the breach ($Z=0$) is inversely proportional to $\dot{I}_0^{1/2}$; hence higher \dot{I}_0 should result in lower initial dwell times and hence less gas evolution in the breach of the coaxial gun (Figure A2).

Parasitic currents occurring in the breach of the 1MJ plasma focus at Frascati^{A8} are believed to be responsible for the lower than expected neutron yields reported for that device with respect to those reported^{A9} for Mather's DPF of similar energy. The Frascati device operated with an \dot{I}_0 of $1.3 \cdot 10^{12}$ A/s whereas Mather's device had an \dot{I}_0 of $3.3 \cdot 10^{12}$ A/s.

An extreme example of the process of parasitic currents occurring in the breach of a plasma gun is the erosion railgun^{A10-A12}. In the erosion railgun the entire working gas evolves from the insulator and electrodes at the breach^{A10}. In these experiments \dot{I}_0 and peak current were^{A12} $3 \cdot 10^{10}$ A/sec and 120 kA respectively which are similar to those of Salge. In the erosion railgun, greater than 50% of the device current remains in the breach region^{A11} and the percentage of total system energy dissipated in the breach was found to decrease^{A10} with bank voltage, V , and to be independent^{A10} of the number of capacitors (bank energy). Since $\dot{I}_0 = V/L_x$ (where L_x is the total external inductance) and since L_x was dominated by the spark gap^{A12} (hence independent of number of capacitors and bank energy) this type of dependence would be expected if the increased dissipation were caused by low \dot{I}_0 .

Thus there is considerable evidence that a minimum \dot{I}_0 is required to keep parasitic currents low in the dense plasma focus and that in Salge's experiment \dot{I}_0 may have been too low. Also large outward pointing electric fields have been found^{A13} crucial to good current sheath formation and these fields are directly proportional to \dot{I}_0 . Only careful measurements of the magnetic field distribution in the device (\dot{B} probe measurements) can answer this question and such measurement were not reported by Salge^{1,2}. We have proposed these types of measurements in the research plan (Figure 2) so the results of this research should be less ambiguous.

Conclusion

Thus while the DPF opening switch experiments performed by Salge were pioneering in nature, insufficient data is provided to determine whether the performance was ever optimized (for capacitive drive) or whether parasitic currents dominated due to the low \dot{I}_0 . To use the results of these experiments as proof that a DPF opening switch concept is impossible is to greatly overstate the case. However one can use the results of Salge's experiments to suggest better modes of operation (e.g., the gas recovery mode and/or the magnetic field stabilized mode) or to suggest more comprehensive experimental tests (e.g., \dot{B} probe measurements) and this is what we plan to do (Figure 2).

Appendix 1)

- A1) J. W. Mather, Meth. of Exp. Phys. 9B (Academic Press, 1971) 238-242.
- A2) G. Decker and R. Wienecke, Physica 82C, 155 (1976).
- A3) D. Turnquist, R. Caristi, S. Friedman, S. Merz, R. Plante and N. Reinhardt, Proc. of 2nd IEEE Pulsed Power Conf., Lubbock, TX, IEEE Cat. No. 79CH1505-7, 17 (1979).
- A4) L. Michel, K. H. Schoenbach and Heinz Fischer, Appl. Phys. Lett., 24, 57 (1974).
- A5) C. M. Fowler, R. S. Caird, D. J. Erickson and B. L. Freeman, Proc. of 3rd. IEEE Pulsed Power Conf., Albuquerque, NM., IEEE Cat. No. 81CH1662-6, 344 (1981).
- A6) B. L. Freeman, R. S. Caird, D. J. Erickson, C. M. Fowler, and H. W. Kruse, 1981 IEEE Int. Conf. on Plasma Science, Conf. Record-Abstracts, Santa Fe, NM, IEEE Cat. No. 81CH1640-2 NPS, 60 (1981).
- A7) T. Oppenlaender, G. Pross, G. Decker and M. Trunk, Plasma Phys. 19, 1075 (1977).
- A8) T. Oppenlaender, "Measurements of Magnetic Field and Current Density Distribution in the Frascati IMJ Plasma Focus Device," C.N.E.N. Report 78.6, Edizione Scientifiche C.P. 65, 00044 Frascati, Rome, Italy (1978).
- A9) K. D. Ware, A. H. Williams and R. W. Clark, Bull. Amer. Phys. Soc. 18, 1364 (1973).
- A10) A. Ya Balagurov, S. D. Grishin, V. L. Levtoy, L. V. Leskov, V. G. Mikhalev, A. M. Petrov, A. F. Savin, V. V. Savichev, and V. A. Chivilev, Sov. Phys.-Tech. Phys. 15, 345 (1970).
- A11) A. G. Kalygin, N. P. Kozlov, L. V. Leskov and V. B. Saenko, Sov. Phys.-Tech. Phys. 15, 355 (1970).
- A12) A. G. Kalygin, N. P. Kozlov, N. A. Koreshchenko, L. V. Leskov and V. B. Saenko, Sov. Phys.-Tech. Phys. 15, 928 (1970).
- A13) G. Decker, W. Kies and G. Pross, Phys. Lett. 89A, 393 (1982).

FSL-82-246

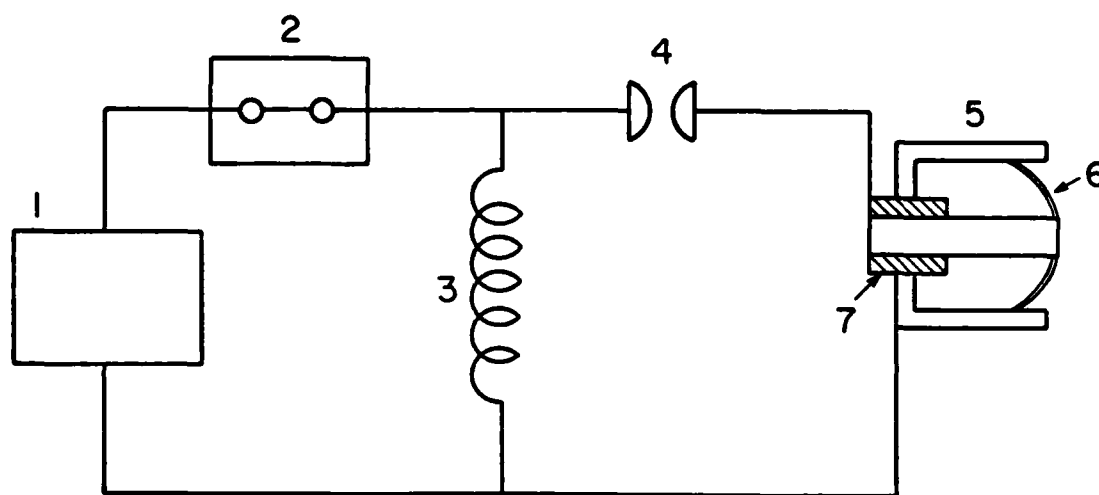


Figure A1: Circuit used by Salge to test the plasma focus as an opening switch. The circuit components are as follows: 1) charging power source, 2) circuit breaker (opens once), 3) storage coil, 4) spark gap (breakdown voltage ~ 20 kV), and 5) plasma focus, where 6) labels the current sheath and 7) labels the insulator.

FSL-82-247

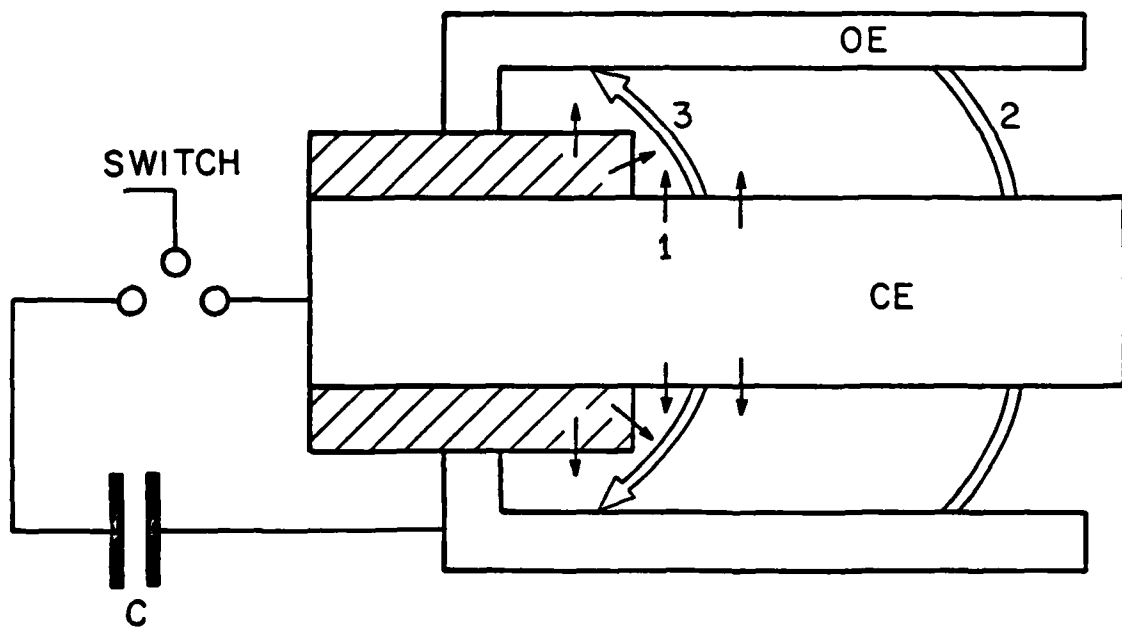


Figure A2: Gas evolving 1) from heated surfaces of insulator and electrodes caused by primary current sheath 2) can lower the breakdown voltage behind this sheath giving rise to a second or parasitic current sheath 3).

Appendix B: Discussion of the goals

The answers to the four questions listed in Section C1 provide the goals required for realizing the potential of the Plasma Focus Opening Switch (PFOS) concept. The ordering of the goals is such as to provide tests of increasing difficulty and yet at the same time opening the concept to a wider range of applications at each step if the result of the previous goal is positive. Thus knowledge of the nature^{B1} of the current interruption in the plasma focus (inductive or resistive) leads to strategies to improve PFOS performance in the subsequent tests of power transfer, control, and rep. rate. Subsequently if little power can be transferred out of the circuit then questions of control and rep. rate are irrelevant. Since each goal depends on the results of earlier goals most of the discussion will be centered on the first goal. The others will be discussed in terms of the most likely results of the earlier goals as perceived at present to show how this research program could lead to a fast reliable opening switch.

The Nature of the PFOS Impedance

It is necessary to determine the nature of the current interruption of the plasma focus before potential loads can be considered or ways of improving performance can be devised. For single shot experiments it is desirable to match source and load impedances to insure the maximum transfer of energy^{B2,B3} and hence switch impedances ranging from 0.5Ω for exploding wire experiments^{B4} to 1 or 2Ω for water transmission line^{B5} experiments would be desired. For a rapidly pulsed system this may not be the optimum since time to replenish the source energy may seriously degrade the rep. rate. However if the energy density of the inductive store can be made a hundred times greater than capacitive stores, interesting pulsed power sources could be envisioned that have rapid rep. rates and that are not prohibitively large.

As an example consider the circuit in Figure B1 where the opening switch S_1 is replaced by a variable resistor which ramps up at a constant rate \dot{R} starting when the power pulse to the inductive load is desired (and S_2 is closed). The power P transferred from inductor L_1 carrying initial current I_1 to the load inductor L_2 can be written^{B2} as:

$$P = \frac{L_1}{L_1 + L_2} 2\dot{R}I_1^2 t (e^{-\beta t^2} - e^{-2\beta t^2}) \quad B1)$$

$$\beta = \frac{\dot{R}(L_1 + L_2)}{L_1 L_2}$$

where t is time starting when \dot{R} is turned on. The total energy transferred to the load up to time t can be written

$$E(t) = \frac{L_1 L_2}{(L_1 + L_2)^2} \frac{1}{2} L_1 I_1^2 [1 - (2e^{-\beta t^2} - e^{-2\beta t^2})] \quad B2)$$

Taking the load to be 6 nH which is of interest in high pulsed power plasma experiments^{B2} and $\dot{R} \sim \frac{150\text{m}\Omega}{150\text{nsec}}$ consistent with parameters of the

Illinois plasma focus the two equations can be used to predict the performance of a PFOS. Two cases were considered: the present experiment where $L_1 \sim 45$ nH and $I_1 = 560$ kA and a high energy inductive energy storage circuit where $L_1 \sim 145$ nH and $I_1 = 10$ MA. The results are shown in Table BI. The data in Table I indicate that a PFOS operating in an inductive energy storage system could deliver power pulses that compare quite favorably with the present SHIVA II implosion experiments at Air Force Weapons Lab in terms of peak power^{B2} and are only a factor of three lower in terms of energy transferred. Also Table BI illustrates that increasing \dot{R} shortens the energy transfer time and that measurable amounts of energy and power could be coupled out of the Illinois plasma focus experiment assuming

\dot{R} is not effected by the transfer of energy. Finally the energy lost to the focus circuit in the switch (i.e. $\int I^2 R_s dt$) is only 1.45 kJ whereas analysis^{A1} of the current waveform (Figure 3) indicates 1/2 of the magnetic energy in the circuit or 3.5 kJ is lost. This could indicate that the Illinois Plasma Focus has a resistance even higher than that used in this study.

Thus the determination of the nature of \dot{R} is a key to the potential use of a plasma focus as an opening switch. For example if \dot{R} is due to a dissipative effect then methods to increase the dissipation rate such as increasing the energy radiated by the use of a high Z working gas could be examined. If the \dot{R} (or \dot{L}) is due to sheath acceleration then methods of increasing the sheath velocity such as the use of hydrogen at low pressures as a working gas would be the local next step.

It should be said at this juncture that earlier plasma focus (27 kJ) circuit and current-sheath velocity measurements^{B6,B7}, indicated that the maximum resistive component was 150 m Ω whereas the inductive (L^*) component was 10 to 20 m Ω when the center electrode is positive. However since the total current interrupted^{B6} was only 10 kA (out of 530 kA) as opposed to 280 kA (out of 560 kA) for the Illinois plasma focus (IPF), similar measurements will have to be performed on IPF to be certain that the resistive component continues to dominate. These measurements will be discussed in detail in the next section, but for the basis of the discussion of the rest of this section it will be assumed that the resistive (dissipative) component dominates the current interruption in IPF (and all other PFOS) as well.

Tapping the Energy into a Load

While this is an obvious next step after determining the nature of the IPF impedance it is interesting to speculate on how the resistive component

might be effected by withdrawing current and power from the plasma focus to suggest possible ways to circumvent such behavior.

As a possible scenario, assume the anomalous resistance of a plasma focus (typically 100X Spitzer) is caused by current driven instabilities which are caused when the electron drift velocity, v_D , (carrying the current) exceeds some typical plasma velocity as the electron thermal velocity v_{Te} or the ion sound speed C_s .^{B8} If current is transferred to the load the resulting lowering of v_D could cause these instabilities to be stabilized (and damped) and hence cause the resistance of the plasma focus to rapidly decrease.

Computer calculations^{B9} based on a one-dimensional Lax-Wendroff two-fluid model including anomalous transport as outlined in reference B8 indicate that conditions should be favorable for current driven instabilities. These instabilities could increase the resistivity of the plasma focus to over one thousand times Spitzer resistivity during the current collapse which is the same order as $R \sim V_p/I_p$ estimated above. If this is truly the dominant mechanism for enhanced resistivity as the above analysis indicates then tapping the power into the load could considerably lower the switch resistance just when high resistance is desired. Clearly some means of circumventing these phenomena would have to be sought.

Another mechanism that would enhance resistivity appears to be occurring in the plasma focus^{B10}. This mechanism is magnetically induced mass motion. Starting with the MHD equation of motion and the generalized Ohm's Law^{B11} the following relation can be obtained:^{B12}

$$\frac{d}{dt} \int \frac{\mu \rho}{\sigma} \vec{v} \cdot d\vec{l} = \frac{d\psi}{dt} + \int \left(\frac{\vec{j}}{\sigma} + \frac{1}{en_e} \vec{\nabla} (p_e - p) \right) \cdot d\vec{l} \quad B3)$$

where the closed loop moves with the fluid. \vec{v} is the fluid velocity; ψ is the magnetic flux enclosed by the loop; μ , ρ , and σ are the mobility, mass density and conductivity of the fluid respectively, and the rest of the notation is standard. Since the integral around the loop of a gradient is zero the last term in equation 3) can be neglected. This equation illustrates that decaying flux can be converted into heat via Ohmic losses or into mass motion. Since the latter also removes energy from the circuit it also represents an effective resistance.

To induce mass flow, one of the constituents of the fluid must be free to move across the magnetic field lines; a figure of merit for this can be expressed in terms of the Hall parameter $\omega_{cj}\tau_j$, where ω_{cj} is the cyclotron frequency for species j and τ_j is the collision frequency for that species. For a typical plasma focus pinch $\omega_{ci}\tau_i < 1$ for the ions and $\omega_{ce}\tau_e \gg 1$ for the electrons so the ions are free to move across the field and be accelerated by a decreasing magnetic flux into the circuit. Since $\mu/\sigma = -1/(|e|n_e)$ the ion motion is away from the center electrode when it is positive and toward the center electrode when it is negative. A solid center electrode would impede mass flow in the latter case and this may explain why a strong shock wave moving away from the center electrode is observed only when it is positive^{B13} and why the resistance of the focus is ten times higher with a positive center electrode than with a negative center electrode.^{B7} This effect might also explain the generation of 1 kJ of fast ions moving away from the center of electrode in the Illinois plasma focus^{B14, B15} with a positive center electrode.

Magnetically induced mass motion (MIM), i.e. the conversion of magnetic energy to mass motion should only be inhibited if the ion Hall parameter increases above one. Since

$$\omega_{ci} \tau_i \propto \frac{BT_i^{3/2}}{n_i}$$

where n_i , T_i , B are the ion number density, the ion temperature and the local magnetic field, ion heating or rarefaction could stop this effect. However tapping the current to a load should also reduce B so the switch resistance may not be effected by including a load. This would be a very promising event in view of the results reported in Table BI.

Thus the plasma focus load experiments might yield both the practical result of coupling energy to a load using a PFOS and also reveal the resistance mechanism which could have important consequences beyond the PFOS concept.

Firing Control

If magnetically induced motion is the cause of the observed resistivity in the plasma focus this may be enhanced by counter streaming electron beams (traveling in the opposite direction to the current carrying electrons in the plasma) to enhance the flux annihilation in the circuit. Since half the magnetic flux being annihilated is that of the circuit this would enhance the resistivity of the main circuit and provide a means of control of the switching process. Alternatively two stream instabilities produced by such a beam could also enhance the resistivity. Strong interactions have been observed between electron beams and plasma focus pinches^{B16,B17} and a factor of five increase in neutron production was observed^{B17} when a 350 kV,

32 kA, 30 nsec electron beam interacted with the focus in the counter current direction. Since the enhanced ion mass flow predicted by equation B3) would produce more fusion neutrons by either a beam target or a thermonuclear mechanism, the observed enhancement in neutron production is consistent with the magnetically induced motion model.

For these reasons electron beam plasma focus interactions appear to be promising means of controlling the properties of the plasma focus opening switch and thus electron beam focus experiments are an important next step after the focus-load experiments. Permission to use a 250 kV, 80 kA and 30 nsec electron beam has been obtained from the Gaseous Electronics Lab at UIUC.^{B18}

Repetitive Operation

If the electron beam plasma focus experiments are successful and the magnitude of the interruption can be controlled by an electron beam, then repetitive PFOS experiments would be the final step. This could be accomplished by either shortening the center electrode so multiple pinches could occur in the first half cycle of the plasma focus current or by driving the plasma focus by an inductive energy store as in the case of Salge.¹ The lack of firing control exhibited in the experiments by Salge may be overcome by an electron beam controlled plasma focus discharge. Other strategies were outlined in Appendix A. Hence the research program proposed here could lead to a design for a high-power repetitive controllable opening switch if the results of each step of the program are positive. Since the goals of each step are well defined the results can be readily evaluated at the end of each step as well.

Appendix B References

- B1. R. J. Harvey and A. J. Palmer, "Opening Switch Technology," Workshop on Repetitive Opening Switches, M. Kristiansen and K-H Schoenbach eds., Texas Tech. U., Lubbock, TX 79409, 313 (1981).
- B2. C. Stuerke, R. E. Henderson, D. L. Smith, R. E. Reinovsky, Proc. of 3rd IEEE Intern. Pulsed Power Conf., Albuquerque, NM., 328 (1981).
- B3. Ch. Maisonnier, J. G. Linhart, and C. Gouylan, Rev. Sci. Instrum. 37, 1380 (1966).
- B4. D. Mosher et al., Appl. Phys. Lett. 23, 429 (1973).
- B5. G. B. Frazier et al., Proc. of 3rd IEEE Intern. Pulsed Power Conf., Albuquerque, N.M., 8 (1981).
- B6. A. Bernard, A. Coudeville, J. P. Garconnet, A. Jolas, J. de Mascureau, C. Nazet, 6th Intern. Conf. on Plasma Phys. and Contr. Nucl. Fusion Res., Berchtesgaden, FRG, III, 471 (IAEA, 1976).
- B7. A. Bernard, A. Jolas, J-P Garconnet, J. de Mascureau, C. Nazet, A. Coudeville and A. Bekiarian, French Atomic Energy Commission Report CEA-R-4807 (1977).
- B8. R. C. Davidson and N. A. Krall, Nuclear Fusion 17, 1313 (1977).
- B9. W. A. Stygar, Ph.D. Thesis, University of Illinois, Urbana-Champaign, (1982).
- B10. E. A. Witalis, Atomkernenergie-Kerntechnik 36, 177 (1980).
- B11. L. Spitzer, Jr., Physics of Fully Ionized Gases, 2nd Ed. (Interscience, 1962) 27-28.
- B12. E. A. Witalis, Plasma Phys. 10, 747 (1968).
- B13. A. Bernard, A. Coudeville, A. Jolas, J. Launspach, and J. de Mascureau, Phys. Fluids 18, 180 (1975).
- B14. G. Gerdin, J. Durham, and R. Ilic, Nucl. Tracks 5, 299 (1981).
- B15. G. Gerdin, "Interim Annual Report 30 Sept. 1980-30 Sept. 1981," Fusion Studies Lab Report FSL-68, Urbana, IL 61801 (1981).
- B16. J. W. Mather, J. P. Carpenter, D. A. Freiwald, K. D. Ware and A. H. Williams, J. Appl. Phys. 44, 4913 (1973).
- B17. D. A. Freiwald, K. R. Prestwich, G. W. Kuswa and E. H. Beckner, Phys. Lett. 36A, 297 (1971).
- B18. J. Verdeyen, private communication.

Table BI

L_1	45 nH	145 nH	145 nH	145 nH
I_1	560 kA	10 MA	10 MA	10 MA
\dot{R}	$10^6 \Omega / \text{sec}$	$10^6 \Omega / \text{sec}$	$3 \cdot 10^6 \Omega / \text{sec}$	$10^7 \Omega / \text{sec}$
P_{MAX}	$0.94 \cdot 10^{10} \text{ W}$	$3.4 \cdot 10^{12} \text{ W}$	$5.9 \cdot 10^{12} \text{ W}$	$10.7 \cdot 10^{12} \text{ W}$
$E_{90\ddagger}$	0.65 kJ	248 kJ	248 kJ	248 kJ
$t_{90\ddagger}$	125 ns	130 ns	75 ns	41 ns
$R(t_{90})\ddagger$	0.125Ω	0.13Ω	0.225Ω	0.41Ω
$1/2 L_1 I_1^2$	12.5 kJ	7.25 MJ	7.25 MJ	7.25 MJ
$\int I^2 R_s dt$	1.45 kJ	425 kJ	424 kJ	424 kJ

†The subscript refers to that quantity when 90% of the energy, E, is transferred to the load.

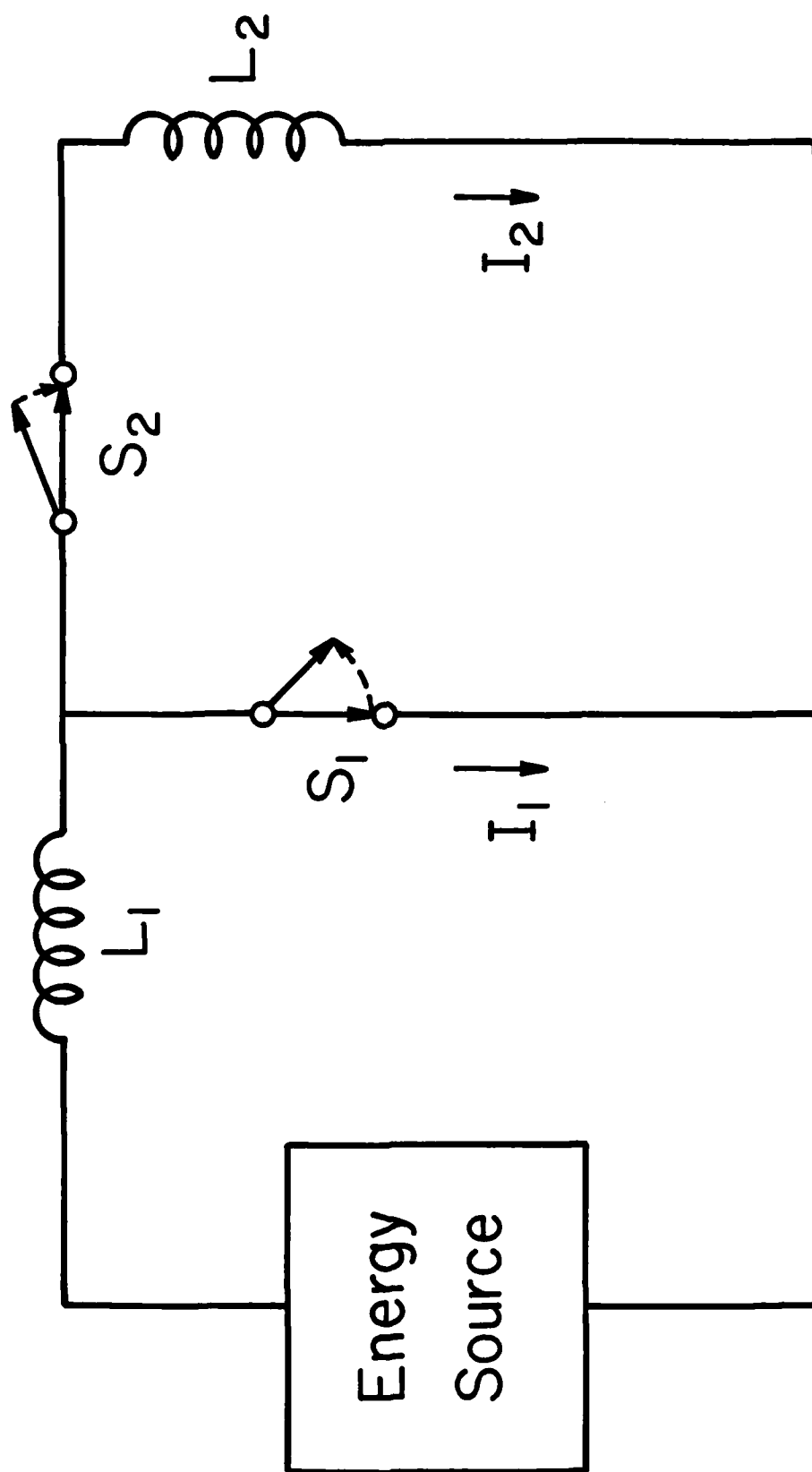


Figure B1: Inductive energy supply circuit. The energy is stored in the inductance L_1 with switch S_1 closed. Ideally the energy would be transferred to load L_2 by simultaneously opening S_1 and closing S_2 .

d) Cumulative Chronological List of Publications

G. Gerdin, W. Stygar, and F. Venneri, "Faraday Cup Analysis of Ion Beams Produced by a Dense Plasma Focus," J. Appl. Phys. 52, 3269 (1981).

G. Gerdin, J. Durham and R. Ilic, "Solid State Nuclear Track Detectors and High Fluences of Light Ions," Nuclear Tracks, 5, 299 (1981).

W. Stygar and G. Gerdin, "High Frequency Rogowski Coil Response Characteristics," IEEE Trans. on Plasma Sci., PS-10, 40 (1982).

W. Stygar, G. Gerdin and F. Venneri, "Particle Beams Generated by a 6-12.5 kJ Dense Plasma Focus," Nucl. Fusion, 22, 1161 (1982).

e) List of Professional Personnel Associated with the Research Effort
Personnel

Glenn Gerdin, Asst. Professor, Nuclear Engineering, Principal Investigator

William Stygar, graduate assistant supported by AFOSR (supported until end of Fall Semester of 1981)

Francesco Venneri, graduate assistant supported by AFOSR

John Mandrekas, graduate assistant supported by AFOSR

Mark Tanis, graduate assistant supported by AFOSR

Advanced Degrees

Jan. 1980, William Stygar, Master of Science in Nuclear Engineering, University of Illinois at Urbana-Champaign, thesis title: "Design, Construction, and Operation of a Fast Rise Time, High Voltage Pulse Generator."

Jan. 1982, William Stygar, Doctor of Philosophy in Nuclear Engineering, University of Illinois at Urbana-Champaign, thesis title: "An Experimental and Theoretical Investigation of Electron Beams Generated by a Dense Plasma Focus."

f) Interactions

Conference Papers

Fall 1980 Meeting of the Plasma Phys. Div. of the Amer. Phys. Soc.:

R. Ilic, G. Gerdin, J. Durham, B. Wehring, W. Stygar, T. Emoto, Bull. Amer. Phys. Soc. 25, 962 (1980).

W. Stygar, G. Gerdin, F. Venneri, Ibid 833.

Spring 1981 IEEE Conf. on Plasma Science at Santa Fe, NM:

W. Stygar, G. Gerdin, F. Venneri, J. Durham and J. Mandrekas, Conf. Record-Abstracts 1981 IEEE Int. Conf. on Plasma Sci., IEEE #81CH1640-2 NPS, 121 (1981).

Fall 1981 Meeting of the Plasma Phys. Div. of the Amer. Phys. Soc.:

G. Gerdin, W. Stygar, and F. Venneri, Bull. Amer. Phys. Soc. 26, 849 (1981).

Spring 1982 IEEE Conf. on Plasma Science at Ottawa, Canada:

J. Mandrekas, F. Venneri, and G. Gerdin, Conf. Record-Abstracts 1982 IEEE Int. Conf. on Plasma Sci., IEEE #83CH1770-7, 117 (1982).

Plasma Focus Workshop held at Univ. of Maryland in conjunction with IAEA Fusion meeting on September 9, 1982 in College Park.

W. Stygar, J. Mandrekas, and G. Gerdin, "1-D computer modeling of a plasma focus including anomalous transport".

Fall 1982 Meeting of the Plasma Phys. Div. of the American Phys. Soc. in New Orleans, LA.

W. Stygar, J. Mandrekas, and G. Gerdin, Bull. Amer. Phys. Soc. 27, 1063 (1982).

G. Gerdin and F. Venneri, ibid, 1064.

Collaboration:

Three day visit with Prof. K. H. Schoenbach at Texas Tech University, January 1982 (see section b).

END